Antigenic determinants driving serogroup-specific antibody response to Neisseria meningitidis C, W, and Y capsular polysaccharides: Insights for rational vaccine design

Pietri, Gian Pietro; Bertuzzi, Sara; Karničar, Katarina; Unione, Luca; Lisnić, Berislav; Malić, Suzana; Miklić, Karmela; Novak, Matej; Calloni, Ilaria; Santini, Laura; ...

Carbohydrate Polymers 341 (2024) 122349

Contents lists available at ScienceDirect

Carbohydrate Polymers

journal homepage: www.elsevier.com/locate/carbpol

Antigenic determinants driving serogroup-specific antibody response to *Neisseria meningitidis* C, W, and Y capsular polysaccharides: Insights for rational vaccine design

Gian Pietro Pietri [a,1], Sara Bertuzzi [b,1], Katarina Karnicar [d,e], Luca Unione [b,c], Berislav Lisnic [a], Suzana Malic [a], Karmela Miklic [a], Matej Novak [d], Ilaria Calloni [b], Laura Santini [f], Aleksandra Usenik [d,e], Maria Rosaria Romano [f], Roberto Adamo [f], Stipan Jonjic [a], Dusan Turk [d,e], Jesús Jiménez-Barbero [b,c,g,h,*,1], Tihana Lenac Rovis [a,**,1]

[a] *Center for Proteomics, Faculty of Medicine, University of Rijeka, Rijeka, Croatia*
[b] *CICbioGUNE, Basque Research & Technology Alliance (BRTA), Bizkaia Technology Park, Building 800, 48160 Derio, Bizkaia, Spain*
[c] *Ikerbasque, Basque Foundation for Science, Euskadi Plaza 5, 48009 Bilbao, Bizkaia, Spain*
[d] *Jožef Stefan Institute, Department of Biochemistry and Molecular and Structural Biology, Jamova cesta 39, 1000 Ljubljana, Slovenia*
[e] *Centre of Excellence for Integrated Approaches in Chemistry and Biology of Proteins (CIPKeBiP), Jamova cesta 39, 1000 Ljubljana, Slovenia*
[f] *GSK, Siena, Italy*
[g] *Department of Organic and Inorganic Chemistry, Faculty of Science and Technology, University of the Basque Country, EHU-UPV, 48940 Leioa, Bizkaia, Spain*
[h] *Centro de Investigación Biomédica En Red de Enfermedades Respiratorias, 28029 Madrid, Spain*

ARTICLE INFO

Keywords:
Glycoconjugates
MenW
MenC
MenY
Neisseria meningitidis
Vaccines

ABSTRACT

Meningococcal glycoconjugate vaccines sourced from capsular polysaccharides (CPSs) of pathogenic *Neisseria meningitidis* strains are well-established measures to prevent meningococcal disease. However, the exact structural factors responsible for antibody recognition are not known.

CPSs of *Neisseria meningitidis* serogroups Y and W differ by a single stereochemical center, yet they evoke specific immune responses. Herein, we developed specific monoclonal antibodies (mAbs) targeting serogroups C, Y, and W and evaluated their ability to kill bacteria. We then used these mAbs to dissect structural elements responsible for carbohydrate-protein interactions. First, Men oligosaccharides were screened against the mAbs using ELISA to select putative lengths representing the minimal antigenic determinant. Next, molecular interaction features between the mAbs and serogroup-specific sugar fragments were elucidated using STD-NMR. Moreover, X-ray diffraction data with the anti-MenW CPS mAb enabled the elucidation of the sugar-antibody binding mode.

Our findings revealed common traits in the epitopes of all three sialylated serogroups. The minimal binding epitopes typically comprise five to six repeating units. Moreover, the *O*-acetylation of the neuraminic acid moieties was fundamental for mAb binding.

These insights hold promise for the rational design of optimized meningococcal oligosaccharides, opening new avenues for novel production methods, including chemical or enzymatic approaches.

1. Introduction

Neisseria meningitidis (Men) is a gram-negative bacterium known for its exclusive pathogenicity in humans, causing invasive meningococcal disease characterized by meningitis or sepsis (Abdelhameed et al., 2016; Ganesh et al., 2017). The disease manifests rapidly, with mild symptoms preceding a rapid onset, resulting in fatalities in 10–20 % of cases, which can exceed 35 % in case of septic shock (Schneider et al., 2007).

* Correspondence to: J. Jiménez-Barbero, CICbioGUNE, Basque Research & Technology Alliance (BRTA), Bizkaia Technology Park, Building 800, 48160 Derio, Bizkaia, Spain.
** Correspondence to: T. Lenac Rovis, Center for proteomics, Faculty of Medicine, University of Rijeka, Brace Branchetta 20, 51 000 Rijeka, Croatia.
E-mail addresses: jbarbero@cicbiogune.es (J. Jiménez-Barbero), tihana.lenac@uniri.hr (T. Lenac Rovis).
[1] Contributed equally.

https://doi.org/10.1016/j.carbpol.2024.122349
Received 27 March 2024; Received in revised form 15 May 2024; Accepted 29 May 2024
Available online 31 May 2024

Based on the chemical structure of their capsular polysaccharide (CPS), *N. meningitidis* is classified into twelve serogroups. The most severe cases are attributed to serogroups A, B, C, Y, W, and X (Purmohamad et al., 2019; Zhu et al., 2012). Among these, serogroups B, C, Y, and W account for approximately 90 % of invasive meningococcal infections. The capsule of these four serogroups contains neuraminic acid (Neu) in the form of N-Acetylneuraminic acid (Neu*p*5Ac) (Colombo et al., 2018). Serogroups B and C consist of Neu*p*5Ac building blocks with α-2,8- and α-2,9-linkages, respectively. In contrast, serogroups Y and W consist of disaccharide repeating units (RUs) with Neu*p*5Ac α-2,6-linked to glucose (Glc*p*) or galactose (Gal*p*), respectively (Harrison et al., 2013) (Fig. 1A).

The Neu family encompasses a diverse group of nine-carbon backbone α-keto acids predominantly found in the animal kingdom as vertebrate-specific glycans. These glycans are commonly located at the termini of surface-exposed cellular glycoproteins and glycolipids. Neu plays a vital role in vertebrates for cellular recognition by interacting with surface receptors. Conversely, it also serves a dual role by masking other recognition sites within the same organism. This masking action reduces the organism's immune response against its own cells. Interestingly, certain pathogens, such as Men, have developed a protective capsule that contains these mammalian-specific sugars (Cavalcante et al., 2021; Eneva et al., 2021; Li & Chen, 2012; Severi et al., 2007). The expression of this capsule enhances the pathogen's survival within the host by using Neu as a powerful mask, significantly diminishing its antigenicity, and allowing it to evade the host's immune response.

O-acetylation is a commonly observed modification in bacterial cell-surface carbohydrates, including Neu-containing CPSs. This substitution has been found to impact the biophysical properties of CPSs, such as molecular conformation and hydrophobicity, thereby influencing the biological function of Neu in bacterial survival. Notably, *O*-acetylation provides several advantages, for example, enhanced resistance to sialidases, which confers dominance against competing bacteria (Mulard, 2018). Furthermore, *O*-acetylation can significantly impact the antigenicity and immunogenicity of CPSs by either masking naturally exposed epitopes or generating new diverging epitopes. For example, partial de-*O*-acetylayion in a MenC-tetanus toxoid conjugate vaccine resulted in notably higher bactericidal titers compared with the fully *O*-acetylated conjugate. In contrast, reduced antibody responses were obtained with the de-*O*-acetylated polysaccharides in conjugated vaccines of serogroups W and Y (Kensinger & Arunachalam, 2022). Except for MenB, all the previously mentioned Men CPSs present partial *O*-acetylation in the Neu moiety. Specifically, in MenC, acetylation often occurs at positions C-7 or C-8, while MenY and MenW possess acetyl esters at C-7 or C-9 (Lee et al., 2009).

While most licensed MenC, MenY, and MenW (MenC/Y/W) vaccines include partially *O*-acetylated polysaccharides, the role of this modification in immunogenicity for the C and W serogroups is non-critical (Mulard, 2018). Clinical data from large MenC vaccination campaigns have demonstrated no significant difference in functional activity between *O*-acetylated vaccines (Menjugate, Menveo, Menitorix, Menhibrix–GSK Vaccines, Menactra–Sanofi Pasteur; Nimenrix–Pfizer) and de-*O*-acetylated vaccines (NeisVac–North American Vaccine Inc., later acquired by Baxter Bioscience) (Berti et al., 2018). Similar observations have been made for MenW vaccines (Gudlavalleti et al., 2007). Conversely, for MenY conjugates, preclinical experiments in mice demonstrated that acetylated CPS induce higher anti-CPS IgG titers and increased bactericidal activity compared to the de-acetylated analogue (Fusco, Farley, Huang, Moore, Michon, et al., 2007).

In addition to *O*-acetylation, other factors such as length and conformation suggest distinct impacts on the immunogenicity of each CPS (Gómez-Redondo et al., 2020; Khatun et al., 2017). For MenC, a trisaccharide consisting of three repeating units (3 RUs) has been proposed as the minimal fragment required for optimal vaccine development (Liao et al., 2015). Similarly, in the case of MenW, a tetrasaccharide with two RUs was identified as the shortest length

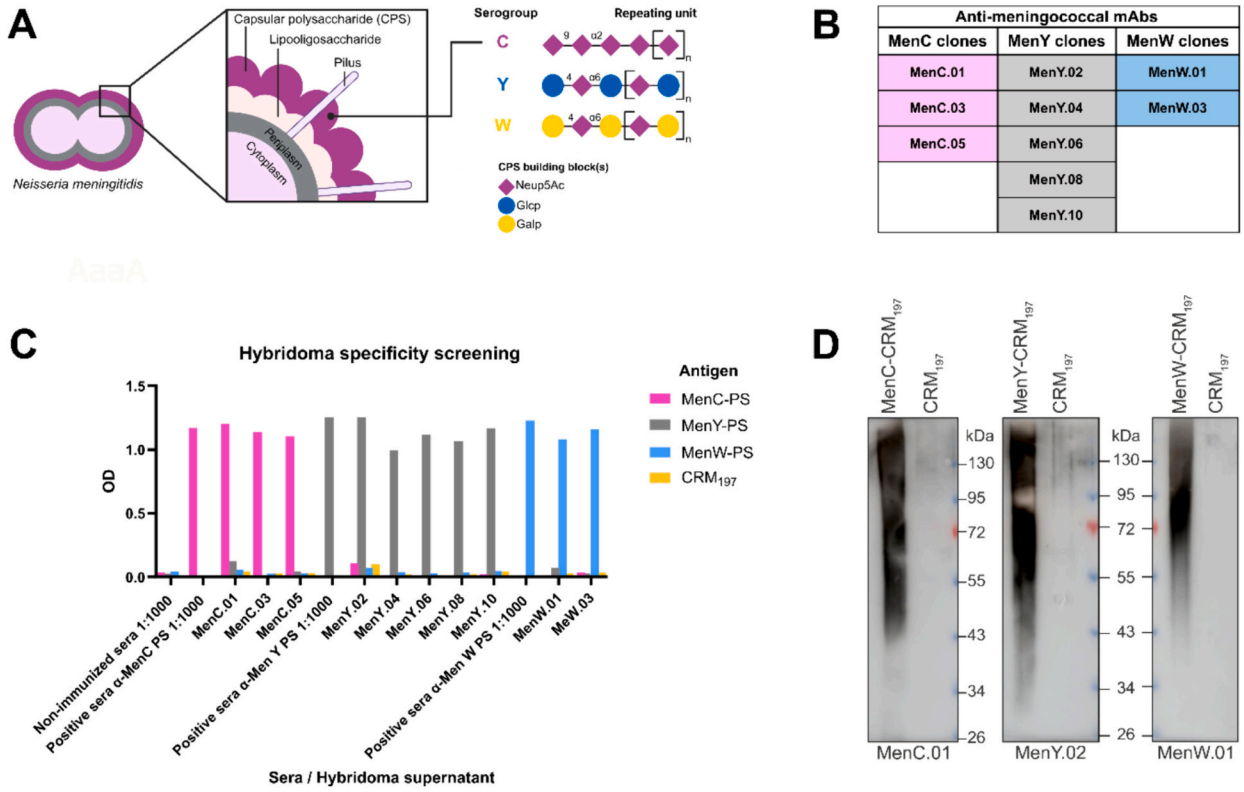

Fig. 1. A. Diagram illustrating *Neisseria meningitidis* bacteria and the key components of the outer layer. Repeating units for MenC, Y, and W CPSs are depicted in brackets. B. Generated monoclonal antibodies (mAbs) corresponding to each serogroup. C. Specificity of the mAbs towards MenC, Y and W polysaccharides. D. Western blot demonstrating mAbs binding to the cognate glycoconjugate, with CRM_{197} used as a negative control.

capable of inducing protective antibodies (Wang et al., 2013). Although the antigenic determinant of MenY has not been confirmed by *in vivo* data, ELISA and NMR studies have suggested that a penta- or hexasaccharide fragment (approximately 2.5–3 RUs) may contain the essential epitope (Moore et al., 2007).

MenC/Y/W polysaccharides share sialylation as a common motif. Typically, meningococcal vaccines contain long polysaccharides, but the minimal length and the chemical moieties responsible for antibody binding are unknown. We hypothesize that the antigenic determinants of MenC/Y/W polysaccharides would be defined in a short glycan with the sialic acid not necessarily *O*-acetylated.

Men CPSs have been used in vaccines for almost 50 years. Initially employed as raw immunogens, modern vaccines utilize glycoconjugates derived either from capsular polysaccharides (CPS) or the corresponding oligosaccharides obtained through hydrolysis. These glycoconjugates are covalently linked to immunogenic proteins, such as tetanus toxoid (TT), diphtheria toxoid (DT) or a recombinant variant of DT, known as cross-reactive material 197 (CRM_{197}) (Berti, 2018; Maiden, 2013; Trattnig et al., 2022). This chemical conjugation improves the anti-carbohydrate immunogenicity, triggering a T cell dependent response, consequently, eliciting a more robust and long-lasting protection in comparison to their non-conjugated version (Anderluh et al., 2022; Micoli et al., 2023). Despite the existence of diverse methods for manufacturing meningococcal vaccines using naturally derived capsular polysaccharides (CPS), the recent demonstration of well-defined synthetic glycans is noteworthy. These glycans are selected based on their interactions with protective monoclonal antibodies (mAbs) and serve as crucial tools for the rational design of new conjugate vaccines. This approach offers enhancements in chemico-physical and immunological features while circumventing the necessity for bacterial growth (Broecker et al., 2016; Enotarpi et al., 2020; Henriques et al., 2020; Kaplonek et al., 2018; Micoli et al., 2019).

To advance the development of next-generation glycoconjugate meningococcal vaccines, we have produced mAbs capable of distinguishing *O*-acetylated Men C, Y, and W CPSs. Our comprehensive approach to elucidate the structural underpinnings of protective short oligosaccharides involves inhibition enzyme-linked immunosorbent assay (inhibition ELISA) and Saturation Transfer Difference NMR (STD-NMR) techniques, complemented by crystal structure data. Notably, our findings underscore the significance of *O*-acetylated groups as critical antigenic features recognized by the protective mAbs. These discoveries pave the way for enhancing the rational design and manufacturing of next-generation meningococcal vaccines, bringing us closer to more effective prevention and control of meningococcal infections.

2. Results

2.1. Generated antibodies successfully discriminate N. meningitidis MenC, MenY, and MenW sugars

Three glycoconjugates, each comprising fragments of meningococcal serogroup C, Y, or W CPS (Fig. 1A), linked to the CRM_{197} carrier protein and prepared as previously reported, were used for immunization (Bröker et al., 2009). CRM_{197} based glycoconjugates were chosen due to its widespread use in commercially available vaccines, such as Menveo [12]. Sera from immunized mice were screened for antibody titers against the immunogen using ELISA and plates coated with respective CPSs. All mice had a high response to MenC, MenY or MenW CPS (Fig. S1). Next, hybridoma technology (Mitra & Tomar, 2021) was used to generate mAb secreting cell lines. The antibodies in hybridoma supernatants were screened by ELISA on MenC, Y or W CPS coated plates. Promising initial hybridomas were isolated through the process of serial dilution, leading to the establishment of stable cell lines that secreted mAbs. Three mAbs were generated for MenC, two for MenW, and five for MenY CPS (Fig. 1B). In total, ten clones specifically recognizing MenC, MenY, MenW were generated.

The specificity of each mAb to their cognate CPS was confirmed by ELISA, which showed high optical density against the target CPS and negative cross-reactivity to other CPSs from the C, Y, W group (Fig. 1C). Furthermore, mAbs immunostaining showed strong signals to CRM_{197}-PS conjugates, but no signal for CRM_{197} protein carrier, ruling out antibody cross-reactivity. A representative immunoblot for anti-MenC, anti-MenW and anti-MenY candidates is shown (Fig. 1D). In conclusion, we have developed a specific set of antibodies that distinguish between Men C, Y and W serogroups.

2.2. Monoclonal antibodies MenC.01, MenY.02, and MenW.01 exhibit strong bactericidal activity

After identifying mAbs capable of selective discrimination among MenC/Y/W CPSs, we investigated their bactericidal activity. The serum bactericidal assay (SBA) has been established as the correlate of protection for Men vaccines, measuring the ability of antibodies to induce killing of *N. meningitidis* in the presence of complement (Acevedo et al., 2017; Micoli et al., 2013). We initially tested the bactericidal activity of the battery of anti-MenC/Y/W mAbs using respective hybridoma supernatants (Fig. 2A). The employed strains were specific to serogroups C, Y, and W: C1, 860,800, and 240,070, respectively. Among the MenC clones, MenC.01, C.03, and C.05 displayed rSBA titers of >2048, <4, and 2048, respectively. For MenW, clones W.01 and W.03 exhibited rSBA titers of 512. Finally, MenY clones Y.02, Y.04, Y.06, Y.08, and Y.10 showed rSBA titers of 2048, <4, 32, 256 and 128, respectively. To eliminate any bias resulting from mAb concentration in hybridoma supernatants, we produced the mAbs with the highest rSBA titers for each serogroup on large scale and purified them for subsequent SBA assays (Fig. 2B). Thus, the anti-MenC/Y/W CPS mAbs, namely MenC.01, MenY.02, and MenW.01, were produced in large quantities and purified. The purified mAbs exhibited rSBA titers of 262,144 (or 0.002 μg/mL) for MenC.01, 131,072 (or 0.004 μg/mL) for MenY.02, and 8192 (or 0.06 μg/mL) for MenW.01, confirming their strong bactericidal performance.

2.3. Oligosaccharides of 5–6 repeating units inhibit binding of bactericidal mAbs, defining a range for their minimal epitopes

To identify the critical residues in the binding of MenC/Y/W antibodies to CPS, we conducted an inhibition ELISA using oligosaccharide (OS) fragments with varying degrees of polymerization (DP), representing the number of monomeric units within the oligomer. DP2, DP5, and DP6 oligosaccharide fragments, representative of MenY and MenW CPS within the previously observed binding range, were used (Moore et al., 2007). For MenC, only DP6 OS was selected, as previous studies have shown it to be the minimal portion that fully inhibits the binding of anti-MenC serum from vaccinated subjects (Costantino et al., 1999; Dalal et al., 2019). The Men mAbs were incubated with increasing concentrations of the OS fragments and then transferred to ELISA plates coated with Men CPS. A negative control without the primary antibody was included.

The inhibition of MenC.01 by DP6 (IC_{50} = 7.49 mg/mL) was compared to that induced by the CPS (IC_{50} = 0.03 mg/mL) at increasing 2-fold dilutions (Fig. 3A). MenC.01 exhibited a 2-log increase in inhibition from DP6 to CPS. Importantly, at 100 μg/mL concentration, DP6 achieved complete inhibition of the interaction, comparable to one obtained with the CPS. In the case of MenY.02, inhibition with DP2 (IC_{50} = 65.32 mg/mL) was increased by 1 log with DP5 (IC_{50} = 8.70 mg/mL), which was comparable to DP6 (IC_{50} = 10.72 mg/mL), and further increased by 2 logs with CPS (IC_{50} = 0.12 mg/mL) (Fig. 3B). Again, although CPS is a more potent inhibitor than DP5, MenY DP5 also exhibits full inhibition at 100 μg/mL concentration. MenW.01 inhibition with DP5 and DP6 was comparable (IC_{50} = 7.65 and 17.14 mg/mL) and increased by 1 log for the CPS (IC_{50} = 1.095 mg/mL) (Fig. 3C). Inhibition by MenW DP2 was very weak, and the determination of IC_{50} was not possible.

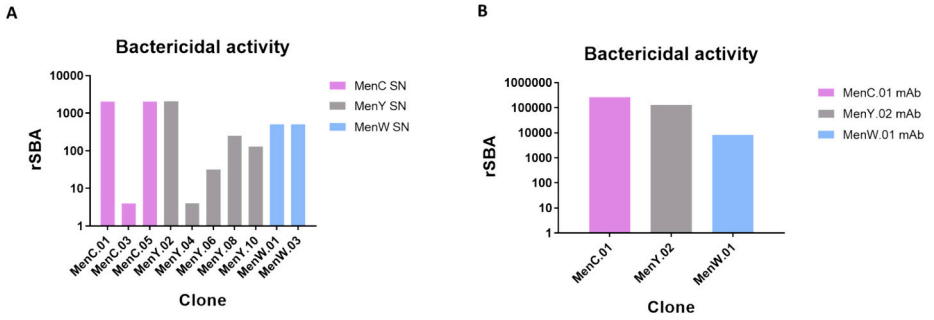

Fig. 2. Serum bactericidal assay for MenC, MenY, and MenW. A. Bactericidal activity of hybridoma supernatants against respective serogroups. B. Bactericidal activity of purified monoclonal antibodies.

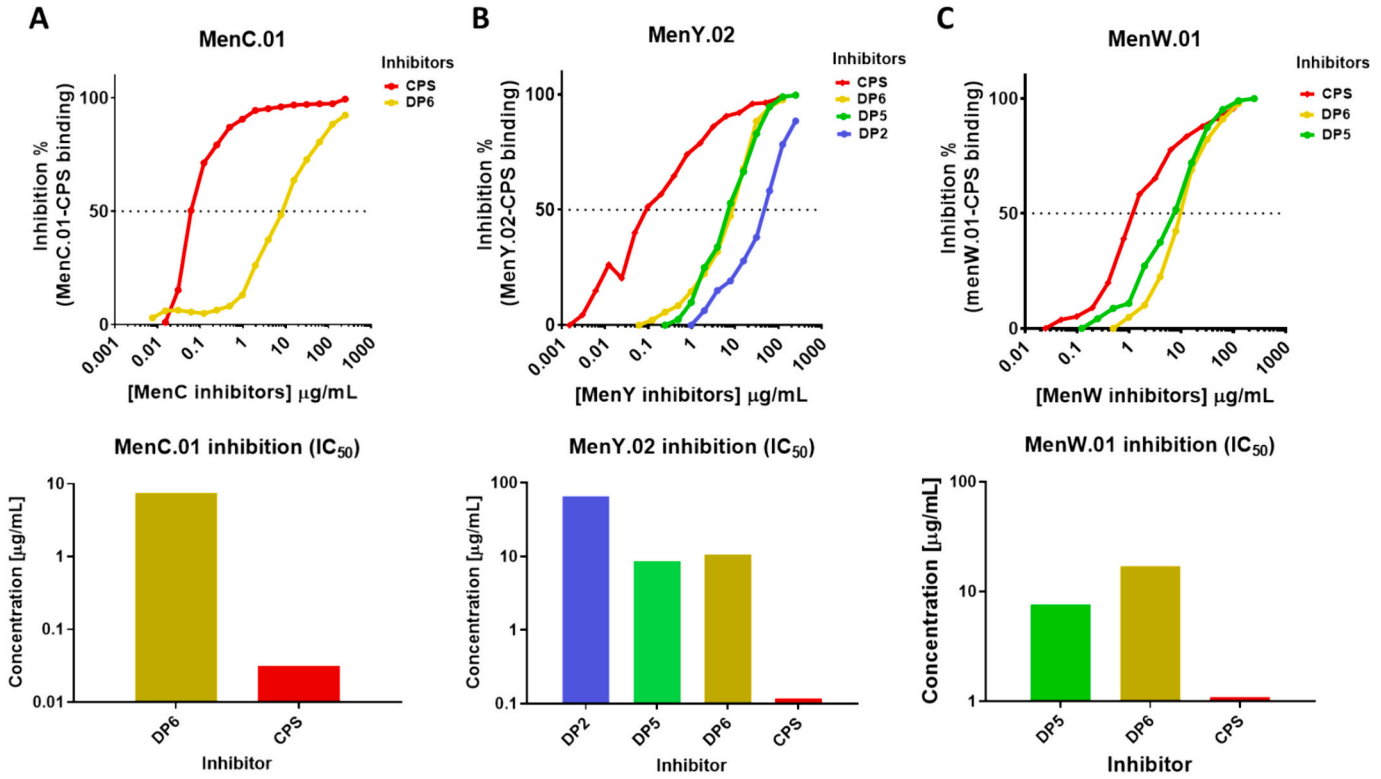

Fig. 3. Inhibition ELISA evaluating mAbs against MenC/Y/W with diverse oligosaccharide lengths. A. Inhibition ELISA (IC_{50}) of specific monoclonal antibodies against native MenC CPS. B. MenY CPS, and C. MenW CPS, used as a coating agent and assessed with Men oligosaccharides of different lengths.

Inhibition ELISA with the newly developed bactericidal anti-Men mAbs confirmed the length-dependent recognition of different fragments. Shorter fragments below DP5/6 were not capable of inhibiting the binding, even at higher concentrations. However, in the case of MenY, it is possible that most of the minimal epitope of MenY.02 mAb is contained within 2 repeating units of the oligosaccharide. In conclusion, these results demonstrated that DP5/6 OS was sufficient to fully inhibit the binding of the mAbs to the native CPS, thereby containing the minimal epitopes.

2.4. MenC, MenY, and MenW CPSs display distinct conformational profiles: disordered and helical structures

Having established that DP5/6 is the optimal OS length for investigating the epitopes of protective anti-MenC/Y/W antibodies, we focused on examining the interactions between these antibodies and their corresponding sugars. First, we initiated a comprehensive structural characterization of the MenC, MenY, and MenW CPS. Given the differences in chemical composition among the three CPSs, it is expected that they possess unique conformations, dynamics, and molecular interaction features (Fig. 4).

To explore the 3D arrangement of the Men CPS structures in solution, a combination of NMR and molecular modeling protocols was employed (refer to Figs. S2-S8 for detailed information). By analyzing experimental Nuclear Overhauser Effect (NOE) NMR data and conducting *in silico* studies, we obtained evidence regarding the conformational behavior of each CPS. The conformational analysis revealed that the MenC CPS exhibited a high degree of flexibility around the glycosidic linkage and the glycerol moiety, resulting in a disordered structure devoid of a marked secondary structural motif. Consequently, the distribution and presentation of *O*-acetyl groups along the polysaccharide chain were stochastic in nature (Fig. 4A). In contrast, the MenY CPS assumed a regular and repetitive geometry, adopting a helix-like structure with four residues per turn. Notably, the acetyl groups at positions 5 and either 7 or 9 of the neuraminic acid residue were exposed to the solvent (Fig. 4B). Similarly, the MenW CPS also adopted a helix-like

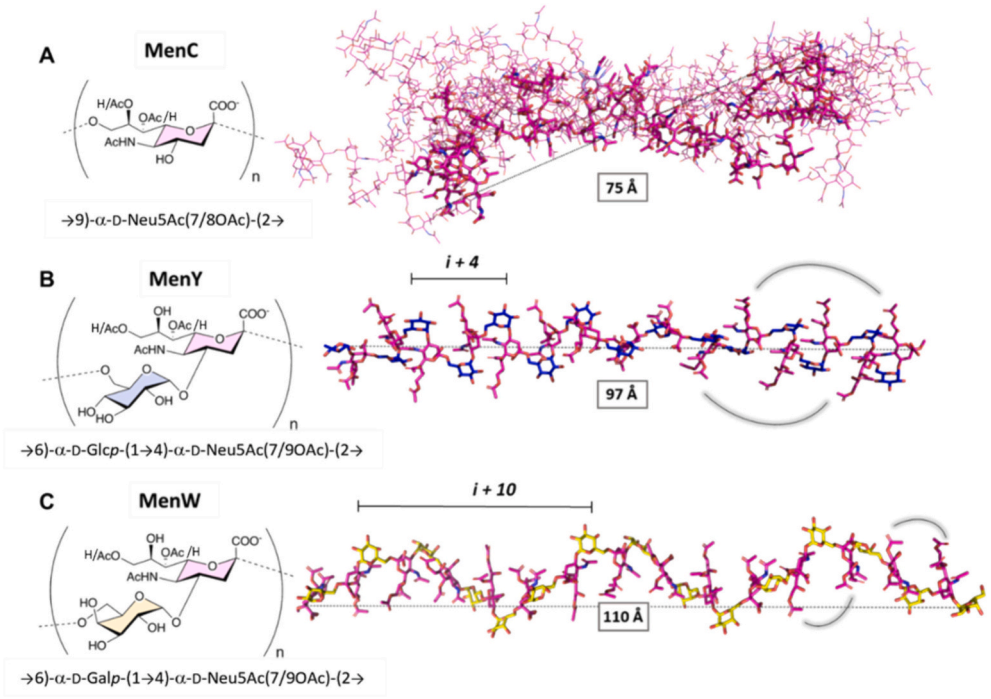

Fig. 4. Chemical structures (*left*) and representation of the major conformations obtained from NMR-based experiments and molecular dynamics (MD) simulations (*right*) of the repeating units for MenC (A), MenY (B), and MenW (C) CPSs. The five most populated conformations of MenC DP30 (A, *right*) are aligned through the central Neu moiety (highlighted in light blue). The most populated structures for MenY and MenW DP15 are reported in panels B and C, respectively. The helix-like structure with a size of four (MenY) and ten (MenW) residues per turn are reported together with the relative orientation of the acetyl groups. (For interpretation of the references to color in this figure legend, the reader is referred to the web version of this article.)

structure, albeit with a more extended helix consisting of ten residues per turn (Fig. 4C). In this case, the acetyl moieties were also exposed to the solvent. To investigate the role of the *O*-acetylation on oligosaccharides 3D structure, we modeled partially acetylated oligosaccharides too, resembling the degree and position of the acetyl groups, as determined by the NMR analysis. The results of this approach suggest that acetylation does not clearly impact the intrinsic 3D structure (Fig. S9). Instead, the difference in helix characteristics between MenY and MenW CPS can be attributed to the rather distinct orientation of the C5-C6 torsion in the α6 glycosidic linkage between gluco- and galacto- configurated sugars, mainly *gauche-gauche versus gauche-trans*, respectively (Fig. S2) (K. N. Kirschner & Woods, 2001).

Overall, the structural studies revealed that the variations in the chemical composition among MenC, MenY, and MenW CPS result in

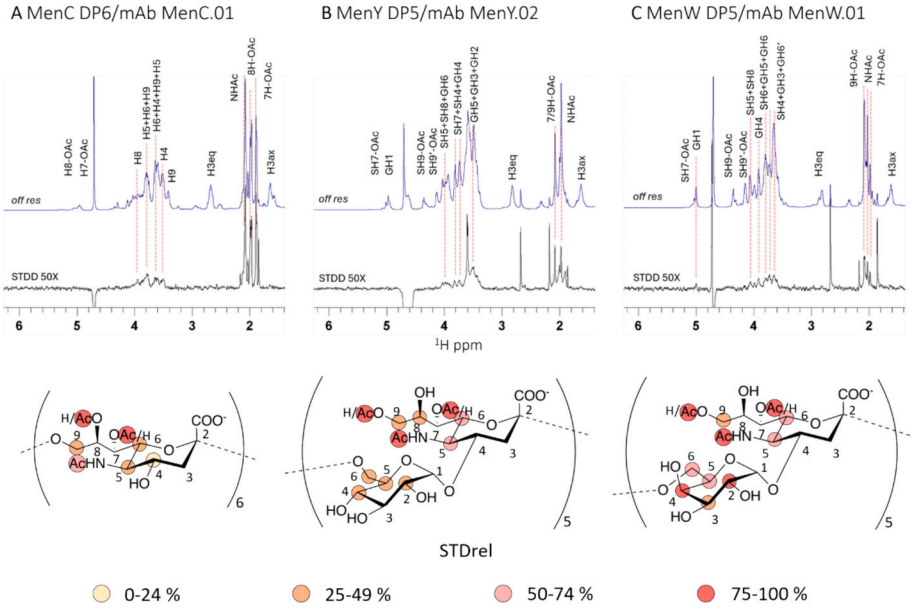

Fig. 5. Epitope maps derived from the analysis of STD-NMR experiments. Top panel. STD-NMR experiments performed for the mixtures of MenC.01:MenC DP6 (A), MenY.02:MenY DP5 (B), and MenW.01:MenW DP5 (C). Bottom panel. The derived epitope maps. The sugar epitopes are represented by spheres, with their relative STD intensities (STD%) indicated. The color legend corresponds to the STD% values, highlighting the degree of interaction between the sugar and the antibody.

distinct conformational dynamics, which are likely to have an impact on molecular recognition.

2.5. STD-NMR spectroscopy highlights the importance of acetyl groups in MenC/Y/W recognition

^{1}H-STD-NMR experiments were conducted to investigate the binding characteristics of MenC (DP6), MenY (DP5), and MenW (DP5) oligosaccharides with their corresponding mAbs at an atomic resolution (Mayer & Meyer, 1999; Valverde, Ardá, et al., 2019; Valverde, Quintana, et al., 2019). The STD-NMR analysis revealed the significance of acetyl groups in the molecular recognition of MenC/Y/W (Fig. 5). In fact, the acetyl groups of neuraminic acid moieties exhibited the strongest saturation transfer signals, indicating their close proximity to the mAbs. Additionally, distinct binding modes were observed among the different serogroups.

In the case of MenC, moderate to weak STD signals were observed for neuraminic acid ring protons (weak for H4, moderate for H5 and H6) and the glycerol chain protons (moderate for H9a and H9b) (Fig. 5A). The acetyl ester methyl protons at C7 or C8, as well as the acetamide methyl protons at C5, displayed the strongest STD signals. Overall, the binding epitope indicated that the interaction between MenC DP6 and the mAb primarily involved hydrophobic interactions of the acetyl groups and the participation of the glycerol chain.

The STD NMR spectrum of the MenY.02/MenY DP5 complex showed a predominant contribution of the Neu and a minor contribution of the Glc*p* to the binding (Fig. 5B). Specifically, the Neu*p*NAc residues predominantly contributed through their acetyl moieties. Medium to strong STD signals were observed for the Neu*p*NAc H5 and H6. The glycerol chain protons H9b, H9a and H8 displayed moderate to weak STD signals, while no STD signals were detected for the H3eq/ax-H4, indicating that this part of the neuraminic acid was not in contact with the antibody surface. Medium to weak ^{1}H-STD signals were observed for the Glc*p* residues (H2, H4, H5, H6R, and H6S). The ^{1}H-STD NMR binding experiments for MenY demonstrated that the acetyl groups of the Neu*p*NAc strongly contributed to the binding, potentially through recognition within a hydrophobic pocket on the antibody surface, while the Glc*p* residues were likely solvent-exposed.

In contrast, the STD-derived results for the interaction between MenW DP5 oligosaccharide and MenW.01 mAb indicated the involvement of both sugar residues, Gal*p* and Neu*p*NAc, in the binding (Fig. 5C). The acetyl groups at the 5, 7, and 9 positions of the neuraminic acid, as well as H2 and H4 of the Gal*p* residues, exhibited the strongest STD contributions. The protons H5, H6, H9a, and H9b of the Neu*p*NAc, along with H5 and H6 of the Gal*p*, displayed medium to strong STD signals. Medium to low STD intensities were observed for the H3 of the Gal*p*, while no STD signals were detected for H8, H7, and H3eq/ax-H4 of the neuraminic acid, indicating their solvent exposure and marginal contribution to the binding.

In conclusion, the STD NMR experiments revealed the distinctive binding modes of the different serogroups to their respective bactericidal antibodies. A common feature observed was the fundamental role of acetyl groups at the neuraminic acid for binding to occur. Furthermore, the distinct nature of the sugar rings (Glc*p* for MenY and Gal*p* for MenW) determined their unique recognition modes. Specifically, in the case of MenW, both the neuraminic acid and galactose residues were found to be in close contact with the antibody-binding pocket, actively participating in the interaction. On the other hand, the involvement of Glc*p* moieties in the binding event of MenY appeared to be comparatively less significant. These findings are in agreement with the different presentation of the Gal*p* (accessible) and Glc*p* (occluded) moieties in MenY and MenW, respectively, as described in the preceding conformational analysis section (Fig. 4 and Figs. S7-S8).

2.6. Fab X-ray crystallography and docking using MenW.01 Fab unveils the intricate binding steps

To determine the precise binding mode of the Men sugars with their respective antibodies, a series of crystallization studies were conducted. To produce suitable antibody proteins for crystallization, variable heavy (VH) and variable light (VL) chain regions were amplified from cDNA transcribed from total RNA of the parental hybridoma clones. The variable regions were cloned in the respective vectors containing the backbone of either the constant heavy chain domain 1 (CH1) or the constant light chain domain (CL). The obtained constructs were used for co-transfection of HEK293T cells, the resulting Fab fragments were purified from the supernatant fraction. Initially, crystallization screening trials were performed with the recombinant fragment antigen-binding region (Fab) alone (Fig. 6) to identify optimal conditions for subsequent co-crystallization. Crystals of MenW.01 Fab suitable for x-ray diffraction analysis were obtained in screen JCSGIII, B5 (0.2 M Na Acet, 0.1 M TRIS, pH 8.5, 30 % *w/v* PEG 4000) (Fig. 6). However, attempts to co-crystallize them with the corresponding MenW oligosaccharide were unsuccessful. Nevertheless, the initial dataset from the crystallization hit was utilized to construct a model (Fig. 7).

Each Fab portion consists of six binding sequences known as complementarity-determining regions, forming a groove along the interface of the variable heavy and variable light chain domains. In the MenW.01 Fab, as many as five of these regions exhibit a neutral or positive charge, indicated by the dominant blue color in Fig. 6.

To gain further insights into the molecular basis of recognition, the MenW decasaccharide (DP5) was docked onto the carbohydrate binding domain (CBD) of the Fab region of the MenW.01 mAb (Fig. 7). The DP5 structure, representing the central section of the DP15 obtained from molecular dynamics simulations (Fig. 4C), served as a representative of the minimal epitope of MenW CPS. The CBD of the MenW.01 mAb features an extended groove flanked by the heavy chain on one side and the light chain on the other. It contains both positively charged and hydrophobic residues, potentially creating salt bridges with the negative carboxylate and hydrophobic interactions with the acetyl moieties of neuraminic acid. Guided by these electrostatic and hydrophobic intermolecular interactions, we docked DP5 onto the CBD. Subsequently, we conducted a docking-minimization protocol for the complex using the MAESTRO (Schrödinger) suite of programs.

In the minimized structure, the terminal region of the decasaccharide starting from the sialic acid moiety Neu5Ac1, known as the reducing end, as well as the central section of the decasaccharide are firmly bound to the mAb through electrostatic interactions between the carboxylate of Neu5Ac1 and Arg98, the carboxylate of Neu5Ac3 and Arg46, and the carboxylate of Neu5Ac5 and Arg32 (Fig. 7). Additionally, polar interactions in the form of hydrogen bonds were observed between Gal2 and His49, and between Gal8 and Arg32. Furthermore, hydrophobic interactions between the acetyl groups of MenW DP5 and the aromatic side chains of Tyr27, Tyr103, Tyr32, Tyr33, Tyr35, Tyr91, Phe96, and Trp50, as well as the aliphatic side chains of Ala102 and Val100, were identified. The last three sugar residues at the non-reducing end appeared to be more flexible, exhibiting only transient intermolecular interactions. The proposed interaction pose aligns with the findings from STD NMR experiments, which indicated significant involvement of the galactose residues and acetyl moieties of the neuraminic acid in protein binding, while the H3eq/ax-H4 of the Neu ring and H7-H8 of the glycerol chain were less engaged in the interaction.

Finally, in an attempt to get a lead of the exquisite specificity of the mAbs against the cognate Men serotypes, we modeled the putative complex between the crystalized MenW.01 Fab and the MenY DP5 (Fig. S10). The resulting structure was compared to that obtained for MenW DP5. While the more extended MenW DP5 is nicely accommodated into the carbohydrate recognition domain of the antibody, the more compact MenY DP5 only marginally binds through the terminal units while leaving the central monosaccharides exposed to the solvent.

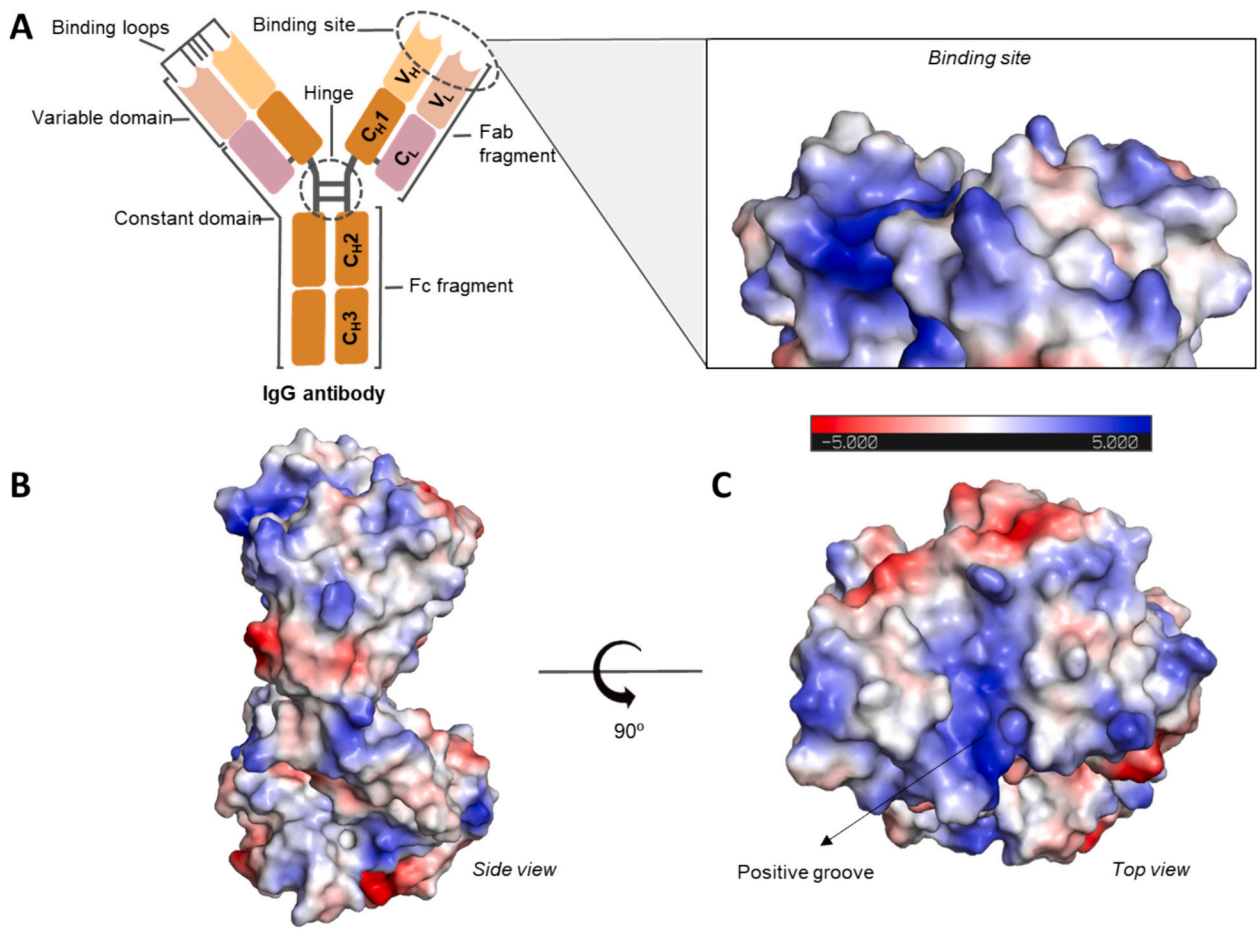

Fig. 6. Structure of an IgG antibody. VH, variable heavy chain domain; VL, variable light chain domain; CL, constant light chain domain; CH1, CH2, CH3, the heavy chain constant domain 1, 2 and 3 (A). Antigen binding site (A), side view (B) and top view (C) of the electrostatic potential distribution of MenW.01 Fab, ranging from −5 kT/e (red) to +5 kT/e (blue). The negatively charged, positively charged, and neutral surfaces are depicted in red, blue, and white colors, respectively. (For interpretation of the references to color in this figure legend, the reader is referred to the web version of this article.)

3. Discussion

In this study, we developed highly specific antibodies targeting the capsular polysaccharides of MenC, MenY, and MenW, and selected a representative bactericidal mAb for each serogroup. Our structural analysis established that the minimal epitope of MenC/Y/W is comprised of five to six RUs (DP5 or DP6). Previous studies have also reported the development of mAbs against these serogroups, such as the antibodies generated by González et al. (González et al., 2019) which included anti-serogroup C (clone 7E12B3), Y (clone 5C11F1) and W (clone 5H10D9) using the Menveo vaccine as an immunogen. Tsang et al. (Tsang & Zollinger, 2005) also produced a similar set of murine mAbs, including clones 4–2-C (MenC), 5–2-Y (MenY) and 7–1-W (MenW), through immunization with whole live bacterial cells. However, only clone 7E12B3 (MenC) (Madariaga et al., 2018) from the aforementioned sets was evaluated for bactericidal activity using serum bactericidal assay, while the bactericidal efficacy of the other mAbs was not assessed. In our study, the obtained bactericidal mAbs belonged to the IgG2a subtype (MenC.01 and MenY.02) and IgG1 subtype (MenW.01), which are commonly observed when glycoconjugates and/or alum adjuvants are used for immunization, as demonstrated by previous authors (Fiorino et al., 2017; González et al., 2019; Liao et al., 2016).

MenC.01 and MenY.02 mAbs demonstrated potent bactericidal activity at very low concentrations, with rSBA titers of 262,144 and 131,072, respectively. The titers, depicted in Fig. 2B, align with those documented for other anti-Men mAbs against diverse serogroups. For instance, an IgG2a mAb (MenA 1.3) specific to MenA capsular polysaccharide exhibited a bactericidal titer of 0.004 μg/mL (Henriques et al., 2020). In contrast, our MenW.01 mAb, which belongs to the IgG1 subtype, displayed an rSBA titer approximately 10-fold lower (0.06 μg/mL). This reduced activity can be attributed to the IgG subtype, as previous studies in mice have established that IgG2 is a more potent activator of the classic complement pathway compared to the IgG1 subtype (Madariaga et al., 2018). Despite the slightly diminished activity, the rSBA titers of these mAbs are well below the minimal protective concentration threshold proposed in our previous research for purified anti-Men mAbs (Pietri et al., 2021). Therefore, achieving these antibody levels in sera through immunization is physiologically attainable.

In order to determine the minimal length of oligosaccharides recognized by the mAbs, we employed Inhibition ELISA. The binding of MenC.01 mAb to MenC CPS was completely inhibited by DP6, indicating that the binding epitope is contained within six RUs. Similar results were observed for MenW.01 and MenY.02 mAbs, where full inhibition was achieved with DP5 sugar fragments. Moreover, the shorter DP2 fragment was unable to fully inhibit the mAb-sugar interaction of MenW.01, although it did show inhibition at high concentrations for MenY.02. These findings are consistent with previous reports, which demonstrated that fragments smaller than two RUs were insufficient to inhibit the binding of rabbit anti-MenW specific sera. Interestingly, MenY oligosaccharide with two RUs had an impact on the binding of the bactericidal anti-MenY mAb, which contrasts with the previous observations made with polyclonal rabbit anti-MenY sera (Moore et al., 2007). This

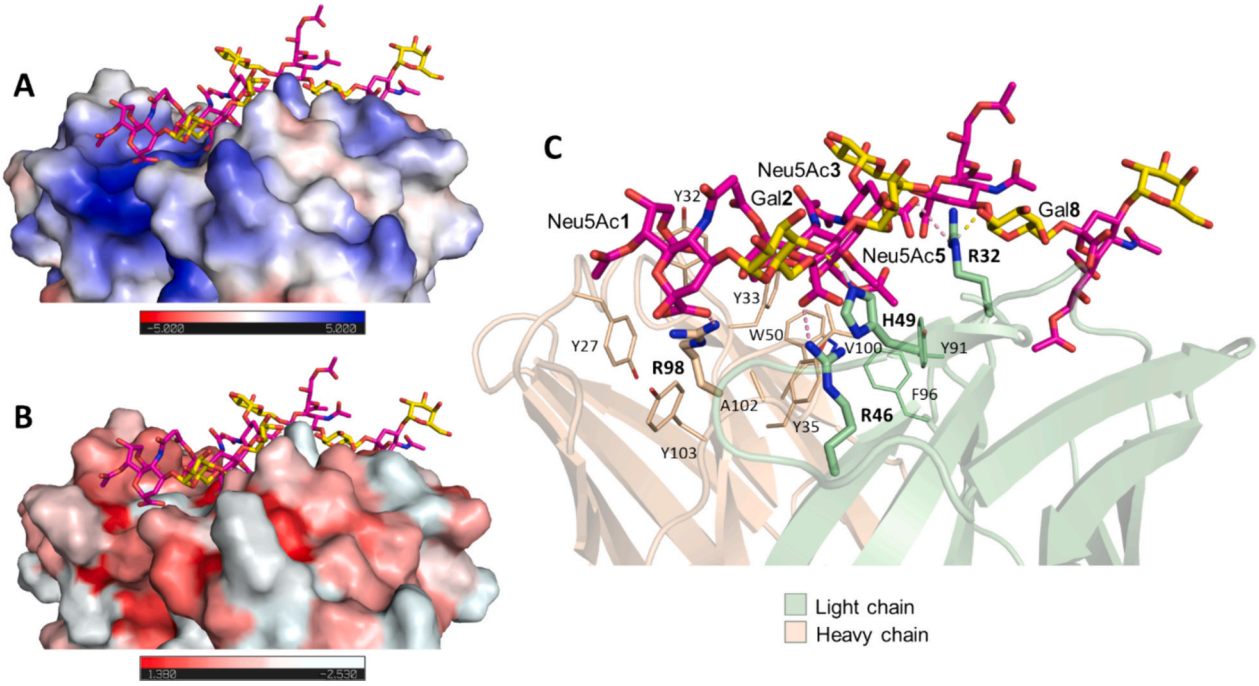

Fig. 7. Docked structure of MenW.01 Fab with MenW DP5 decasaccharide. (A) The potential electrostatic surface displays negatively charged, positively charged, and neutral residues in red, blue, and white colors, respectively. (B) The hydrophobic distribution of the mAb is illustrated in the figure, where red color indicates a more hydrophobic surface, and white color represents hydrophilic regions. (C) The intermolecular interactions of the complex are highlighted, as well as the amino acids that participate in binding. (For interpretation of the references to color in this figure legend, the reader is referred to the web version of this article.)

disparity can be attributed to the more variable and less defined binding observed with the polyclonal serum.

Earlier studies suggested the presence of distinct preferential conformations due to diverse rotamer preferences in the primary alcohol group of Gal and Glc in MenW and MenY CPSs (Fiorino et al., 2017). It was later proposed that MenY CPS displayed one single dominant geometry, whereas MenW exhibited conformational averaging among diverse conformers (Kuttel et al., 2017). We have herein experimentally demonstrated that MenC CPS is characterized by a large ensemble of conformations, leading to a disordered structure. In contrast, MenY and MenW CPS display a higher degree of order, primarily adopting helix-like structures that expose the acetyl groups towards the solvent. Notably, MenW CPS exhibits a more extended structure compared to MenY CPS. Consequently, the Gal*p* rings of MenW were more accessible, while the Glc*p* rings in MenY were occluded within the glycerol chains of the adjacent Neu5Ac residues.

We found that such conformational differences also play a pivotal role in the observed specificities of mAb binding to Men CPSs. The STD-NMR data herein have revealed that, for MenW CPSs, the galactose moiety exhibits close interactions with the antibody, unlike the glucose moiety of MenY. The structural dissimilarity between MenW and MenY CPSs is primarily attributed to the C-4 stereocenter, which significantly influences CPS conformation and antibody recognition. NMR-based conformational analysis, complemented by *in silico* studies, have shown that while both MenW and MenY adopt a helix-like conformation, this structural variation results in distinct helix turns (Fig. 4) that have a substantial impact on epitope exposure and, consequently, recognition.

This study contrasts previous findings suggesting *O*-acetylation in Men CPSs influences the immune response towards non-bactericidal epitopes (Fusco, Farley, Huang, Moore, et al., et al., 2007). Our integrative approach underscores the significant role of *O*-acetyl groups, along with conformational features, in binding Men serogroups C, Y, and W capsules to bactericidal mAbs. While STD-NMR analysis confirmed the presence of few *O*-acetylated epitopes, it emphasized the significance of all acetylation positions, particularly C-8 exclusive to MenC and C-9 characteristic of MenW and MenY. Further investigation into the precise position and percentage of *O*-acetylation is necessary to understand its impact on binding. This requires libraries of sialylated glycans with defined *O*-acetylation patterns, as the heterogeneity of natural fragments limits this study.

This study highlights the minimal antigenic determinant as being within the length range of 5–6 RUs for the three sialylated Men CPSs. However, translating this finding into an effective epitope necessitates further investigation. A variety of short glycan epitopes from different bacterial species have been recently shown sufficiently immunogenic in animal models upon conjugation to a protein carrier (Emmadi et al., 2017; Kaplonek et al., 2018; Martin et al., 2013; Oldrini et al., 2020; Pietri et al., 2021; Schumann et al., 2017), although, to increase avidity of the antibodies generated to the glycan epitope, a fragment longer than the minimal antigenic determinant was preferred for the Shigella 2a synthetic vaccine currently in clinical trials (Cohen et al., 2021; Vulliez-Le Normand et al., 2008). Use of non-conventional carriers or nanoparticles could also be a means to exploit short glycan epitopes (Khatun et al., 2021; Safari et al., 2012).

Overall, these findings have important implications for vaccine design, providing valuable insights that can contribute to the development of more precise and targeted vaccination strategies using innovative chemical and enzymatic technologies.

4. Materials and methods

4.1. Development of mAbs against anti-Neisseria meningitidis serogroups C, Y & W, clones MenC.01, MenY.02 and MenW.01

Individual glycoconjugates of the *N. meningitidis* serogroups C, Y and W CPS with the CRM_{197} carrier protein (MenC/Y/W-CRM_{197}) (GSK, Siena, Italy) were used for BALB/c mice immunization (in groups of two or three female mice). Immunogens were prepared by mixing the MenC/Y/W-CRM_{197} stock [2 μg polysaccharide content, diluted in phosphate-

buffered saline (PBS)], with Alhydrogel® adjuvant 2 % (aluminum content: 9–11 mg/mL) in a 1: 9 alhydrogel: MenPS-CRM_{197} ratio. The immunogen was prepared on the day of immunization and gently mixed at room temperature (RT) for 4–5 h. Mice were subcutaneously immunized with the Men-CRM_{197} conjugate and Alhydrogel® adjuvant two times, at day 0 and 14. Two weeks after the second immunization, the sera were screened for mAbs titers against the MenC/Y/W CPS (GSK, Siena, Italy). The mouse with the highest titer in each group was boosted one more time with the immunogen. Three days after the boost, spleen cells were collected, and after lysis of red blood cells, fusion with Sp2/0 myeloma cells at a ratio of 1:1 was performed. In total, approx. 70 million lymphocyte cells were fused with 70 million fusion partner cells (Sp2/0) and plated on 6 × 96-well plates. These hybridoma cell lines were cultured in 20 % RPMI 1640 medium containing hypoxanthine, aminopterin and thymidine for hybridoma selection. Cell growth was examined 2 weeks after fusion when supernatants were screened by ELISA against Men C/Y/W CPSs and positive hybridoma motherwells were propagated. The hybridoma motherwells were retested the next day, and those with retained positivity against MenC/Y/W CPS were subsequently expanded and cloned by limiting dilution. Obtained cell lines were cultured and retested for their positivity against 1) MenC/Y/W-PS, 2) MenC/Y/W-CRM_{197} conjugate, and 3) protein carrier, CRM_{197} (GSK, Siena, Italy).

4.2. Production and purification of monoclonal antibodies

Large-scale production of anti-Men mAb was performed in RPMI 1640 media (PANBiotech GmbH) supplemented with fetal bovine serum (FBS) standard (PAN-Biotech GmbH) (10 %), penicillin–streptomycin (PAN-Biotech GmbH) (penicillin 100 U/mL; streptomycin 100 μg/mL), L-Glutamine (PAN-Biotech GmbH) (2 mM), and β-mercaptoethanol 50 mM in PBS (PAN-Biotech GmbH) (50 μM). When hybridoma cells reached confluence, the cells were collected and centrifuged, and the medium was replaced with a serum-free medium. After the next 7 days, the medium was collected and the mAb was purified from the supernatant using an AKTA Pure Liquid Chromatography System (Cytiva) and HiTrap Protein G HP (Cytiva) prepacked columns in an amount of a few milligrams. Quality control was conducted using Coomassie staining, as the expected molecular weight (MW) of the mAb is approximately 150 kDa under nonreducing conditions. Under reducing conditions, bands at 50 and 25 kDa were obtained for the MWs of heavy and light chains, respectively.

4.3. ELISA

Microtiter plates (96 wells, MICROLON® High Binding, Greiner Bio-One) were coated with polysaccharides (MenC-PS, MenY-PS or MenW-PS), glycoconjugate MenC/Y/W-CRM_{197}, or CRM_{197} protein. 100 μL of CPS (5 μg/mL) in PBS pH 8.2 or 50 μL of glycoconjugate/protein (2 μg/mL) in carbonate/bicarbonate coating buffer pH 9.6 were added in each well. Plates were incubated overnight at 2–8 °C, washed two times with tap water, and saturated with 150 μL/well PBST-B [3.0 % bovine serum albumin (BSA) in PBST (0.05 % Tween-20 in PBS pH 7.4)] for 1 h at 37 °C. The plates were washed twice with tap water. The coated plates were incubated with mAb or Fab thereof in various dilutions at RT for 1 h, washed twice, and incubated for 1 h at RT with either anti-mouse IgG (H + L) Fc peroxidase (Jackson ImmunoResearch) diluted 1:1000 or anti-mouse IgG F(ab')2 peroxidase (Jackson ImmunoResearch) 1:1000 diluted in PFT (1 % FCS in PBST). After washing six times, the plates were developed with a 0.6 mg/mL solution of *O*-phenylenediamine dihydrochloride (OPD) (Sigma) in citrate buffer pH 5.5 and 0.001 % of 30 % hydrogen peroxide at RT for 5–10 min. After stopping the reaction with 50 μL/well of 1 M sulfuric acid, the absorbance was measured using a TriStar LB 941 multimode microplate reader (Berthold Technologies GmbH & Co.KG). ELISA inhibition experiments were performed following the same procedure but preincubating the samples with one or more concentrations of the inhibitor for 20 min at RT. The OSs preparation, purification, and DP determination were performed as follows: the native MenC/Y/W CPs were subjected to acid hydrolysis in sodium acetate buffer (pH 4.7) for about 7 h at 73 °C. The mixture was then desalted by tangential flow filtration, and the resulting mixtures containing fragments of varying lengths were separated by anionic exchange chromatography (Q Sepharose) using a 50–500 mM NaCl linear gradient elution. Fragment length determination was performed by profiling the single fractions using HPAEC-PAD with a Dionex ICS3000, employing a CarboPac PA200 column and a NaNO3 gradient in 100 mM NaOH.

4.4. Western blot analysis

CRM_{197} protein or MenC/Y/W-CRM_{197} glycoconjugates in the amount of 2–10 μg were separated by 8 % SDS-PAGE. Fab fragments, after their production and purification, in the amount of 2–10 μg were separated by 10–12 % SDS-PAGE. Samples were transferred onto a 0.45 μm PVDF membrane (Hybond™, GE Healthcare), which was subsequently blocked with 5 % *w/v* blotting grade low-fat powdered milk (Carl Roth Gmbh & Co. Kg). Membranes were incubated with Men antibody (mAb or Fab) overnight at 4 °C. We used our own stock antibodies at a concentration of 1 mg/mL with a typical dilution of the primary antibody being 1:100. Protein signals were developed using anti-mouse IgG F(ab')2 peroxidase (Jackson ImmunoResearch) 1:1000 and visualized with an ImageQuant LAS 4000 mini camera system (GE Healthcare). Fab fragments were developed with either anti-mouse IgG F(ab')2 peroxidase (Jackson ImmunoResearch) diluted 1:1000 or anti-mouse IgG (H + L) Fc peroxidase (Jackson ImmunoResearch) diluted 1:1000 to confirm the absence of the Fc fragment in the preparation.

4.5. Complement-mediated bactericidal activity

Serum bactericidal activity against Men strains C1, 860,800, 240,070 were used for evaluating serogroups C, Y and W, as reported elsewhere (Giuliani et al., 2005), with minor modifications. Briefly, bacteria were grown overnight on a chocolate agar plate (Biomerieux) at 37 °C in 5 % CO_2. Colonies were inoculated in 7 mL of Mueller–Hinton broth containing 0.25 % glucose to an optical density at 600 nm (OD_{600}) of 0.05–0.06 and incubated at 37 °C with shaking until the early log phase [OD_{600} of ~0.25 corresponding to 10^9 colony- forming units per mL (CFU/mL)]. The cultured bacteria were diluted in Dulbecco's PBS (DPBS) (Sigma-Aldrich) containing 1 % bovine serum albumin (BSA) (Sigma-Aldrich) and 0.1 % glucose at a working dilution of 10^4–10^5 CFU/mL. SBA was run in round-bottom 96-well microplates in a final volume of 50 μL per well with 25 μL of serial two-fold dilutions of the test sample (supernatants and purified mAbs), 12.5 μL of bacteria under the working dilutions, and 12.5 μL of the active complement (25 %). The assay contains two internal controls: the first is for evaluating the bacterial killing by the complement alone in the absence of antibodies, and the second is for evaluating the killing by supernatant/mAb alone in the presence of a heat-inactivated complement. The reaction mixtures were incubated at 37 °C for 60 min with 5 % CO_2; then, each sample was spotted on Mueller–Hinton agar plates. Serum bactericidal titers were defined as the supernatant/mAb dilution resulting in 50 % decrease in colony-forming units per milliliter after 60 min (time 1) incubation of bacteria with the mixture of complement plus mAb compared with the control (only complement) for colony-forming units per milliliter at time 0.

4.6. Production of recombinant Fab fragments

4.6.1. Preparation of cDNA from hybridoma cells

Construction of the plasmids for recombinant Fab expression was adapted from Nettleship et al., 2008 (Nettleship et al., 2008). Briefly, approx. 1-2 × 10^6 hybridoma cells were pelleted and lysed using TRI

Reagent® solution (Sigma-Aldrich). Total RNA was extracted by adding 100 μL of 1-Bromo-3-chloropropane (Sigma-Aldrich), the mixture was then incubated at RT for 5 min followed by centrifugation at 4 °C for 15 min at 12000 g. The aquatic phase containing the RNA was collected and transferred into a new tube, 500 μL of isopropanol were added, the tube was incubated for 5 min at RT and centrifuged at 4 °C for 10 min at 12000 g. Next, all the supernatant was removed and 1 mL of 75 % EtOH was added, the tube was centrifuged at 4 °C for 5 min at 7500 g. The supernatant was removed, and the pellet was dried at RT. Finally, the pellet was dissolved in 50 μL of RNAse free water and incubated at 55 °C for 10 min. Then, 10 μg of the isolated RNA were treated with DNase I (RNase-free) (New England Biolabs) to remove any DNA in the sample following the manufacturer's protocol. Next, the RNA was loaded into a 1 % agarose 1 % bleach TAE gel and run at 100 V to analyze the RNA quality. RNA was reverse transcribed into cDNA using ProtoScript® II First Strand cDNA Synthesis Kit (New England Biolabs) using an oligo-dT primer [d(T)23VN] and the ProtoScript II Reverse Transcriptase following the manufacturer's protocol.

4.6.2. Preparation of VH and VL flanking with enzyme restriction site

cDNAs encoding the antibody variable heavy and light chains were PCR amplified using reverse primers VH Rev2 POPINVH (5'-GGGTGTCGTTTTGGC) and VL Rev2 pOPINVL (5'-TGCAGCAT-CAGCCCG) which anneal to IgG C_H1 and C_k sequences respectively. The forward primers VH Fwd1 pOPINVH (5′- TGGGTTGCGTAGCT-SAGGTGMAGCTGSARSAGTC) and VH Fwd2 pOPINVH (5'-TGGGTTGCGTAGCTSAGGTGMAGCTGSTKSAGTC) are degenerate primers that anneal to the framework region (FR1) of most murine antibody heavy chain genes. Similarly, VL Fwd pOPINVL (5'-TGGGTTGCGTAGCTGAYATTGTGMTSACMCARWCTCC) anneals to the FR1 of murine antibody κ chain. The 50 μL PCR mixture contained 500 ng of template cDNA, primers and individual dNTP's concentrations were 0.2 μM and 200 μM respectively. Taq DNA polymerase (1.25 U, New England Biolabs) was chosen to catalyze the PCR because it has no proofreading activity that could degrade PCR primers and because it has a dramatic ability, beyond that of other polymerases, to tolerate mismatches between degenerate primers and the template. The PCR program was composed of 30 cycles, with each cycle consisting of three steps (denaturation step at 94 °C for 1 min, annealing at 50 °C for 1 min, and elongation at 72 °C for 1 min). A final elongation step was at 72 °C for 10 min after completion of the 30 cycles. In the case of VL gene amplification, PCR products were digested with *Bci*VI restriction enzyme (New England Biolabs) to eliminate any aberrant kappa chain gene deriving from the Sp2/0 fusion partner. VL BciVI digested and VH PCR products were loaded into a 1.25 % agarose gel and subjected to electrophoresis at 90 V. Next, gel bands around 360 bp (inserts) were excised and DNA was purified using a NucleoSpin® Gel and PCR Clean-up kit (Macherey-Nagel).

4.6.3. Preparation of plasmid DNA

Mammalian expression vectors pOPINVH and pOPINVL were obtained from Addgene as bacterial inoculums (Nettleship et al., 2008). Each inoculum was grown in 5 mL of LB media supplemented with 100 μg/mL of ampicillin at 37 °C for 16–18 h. This culture was used as a starting material for plasmid DNA isolation using NucleoSpin™ Plasmid EasyPure Kit (Macherey-Nagel). The isolated plasmid was used for transformation of XL1 *E. coli*.

4.6.4. Cloning of amplified VH/VL into pOPINVH/pOPINVL expression vectors

Destination vectors pOPINVH and pOPINVL ((Nettleship et al., 2008), Addgene) were linearized for in-fusion cloning with either *Kpn*I/*Sfo*I or KpnI/*Sac*I-HF, respectively and the 6 k bp band was purified following the same protocol as used for the inserts. The 5 μL in-fusion reaction contained 10 ng of DNA insert, 60 ng of linearized vector and 1 μL of In-fusion HD Enzyme Mix (Takara Bio). The cloning reaction was used for transformation of Stellar™ Competent Cells (Takara Bio) by heat shocking the cells for 45 s at 42 °C, followed by addition of SOC medium (Takara Bio) and incubation for 1 h at 37 °C. Transformed bacteria were plated in BD Difco™ LB Broth, Miller (Luria-Bertani) (Becton, Dickinson and Company), agar plates supplemented with ampicillin (100 μg/mL), isopropyl thiogalactoside (IPTG) FC 0.1 mM and 5-bromo-4-chloro-3-indolyl-beta-D-galactopyranoside (Xgal) (Carl Roth) FC 40 μg/mL and incubated overnight at 37 °C. Individual white colonies were inoculated in 3–5 mL of LB media supplemented with ampicillin and incubated for 18 h at 37 °C. Plasmid DNA was isolated from bacterial cultures using NucleoSpin™ Plasmid EasyPure Kit (Macherey-Nagel). Colony PCR was performed using the forward primer T7 (5′- TAATACGACTCACTATAGGG) and either VL Rev. or VH Rev. Primer. Bands of 638 bp confirmed the presence of the 380 bp target insert.

4.6.5. Sequencing of recombinant Fab fragments

To determine the VH and VL sequences of functional MenC/Y/W clones, at least 250 ng of plasmid DNA of each pOPINVH/VL constructs were sent for sequencing services to Eurofins Genomics GmbH (Germany) using their in-house T7 forward primer. Sequencing data were analyzed using SnapGene v.5.3.2 software package.

4.6.6. Expression and purification of the recombinant Fab fragments

Transient expression of recombinant Fab was performed in a mono-, tri-, or five-layer cell culture flask (Corning™ Falcon™ Fischer Scientific). HEK293T cells in RPMI 1640 media (PANBiotech GmbH) supplemented with FBS standard (PANBiotech GmbH) (10 %), MEM NEAA (100×) (PAN-Biotech GmbH), and sodium pyruvate (PAN-Biotech GmbH) FC 1 mM were seeded 24 h before transfection to achieve an 80 % confluency the next day. For each flask layer, the transfection mixture was prepared by mixing 19 μg of each heavy and light chain purified plasmid, 185 uL of polyethylenimine (PEI) solution (1 mg/mL), and 2.8 mL of Dulbecco's modified Eagle's media (PAN-Biotech GmbH) for 20–30 min at RT. Next, the flask medium was removed, and the transfection mixture was added; after incubating for 2 min, the removed media was returned to the culture flask and placed back in the incubator. After 24 h, the medium was exchanged with HyClone™ HyCell TransFx-H medium (Cytiva), collected and replaced every 3–5 days for 1–2 weeks. The recombinant mouse Fabs were purified with HisTrap HP columns packed with Ni Sepharose affinity resin. Fab was analyzed by ELISA and western blot to confirm specific binding to Men CPS.

4.7. Fab crystallization

MenW.01 Fab was concentrated in the range of 5–15 mg/mL. Crystals were obtained using the vapor-diffusion technique in sitting drops as described elsewhere (Lindič et al., 2020; Pintar et al., 2020; Usenik et al., 2017). Briefly, 1 μL aliquot of the protein solution was mixed with 1 μL of reservoir solution containing 0.1 M sodium acetate pH 5.0, 0.2 M sodium chloride, 20 % w/v PEG 6000, followed by drop equilibration at 20 °C over 350 μL of reservoir solution. Crystals were harvested after 14 days, and flash cooled in liquid nitrogen. X-ray data was collected at the ELETTRA synchrotron (Triste, Italy). Refinement and manual model building were performed using Phenix (Liebschner et al., 2019) and COOT (Emsley & Cowtan, 2004), respectively. Data collection and refinement statistics are contained in the validation report (supplemental information). Structure quality was assessed using Molprobity and the reflection and coordinate files submitted to the Protein Data Bank (PDB entry code 8S6E).

4.8. NMR experiments

General considerations: the ^{1}H and ^{13}C NMR signals of the Men C/W/Y OS were assigned through the combined use of 1D and 2D NMR experiments (^{1}H—^{13}C HSQC, TOCSY, NOESY), Figs. S3–5. In particular,

NOE-based experiments were carried out to estimate key proton-proton distances which, along with the analysis of *J* couplings, were used to derive the 3D structures adopted by the molecules in solution. Analysis of the intra-residue NOE and *J* coupling demonstrated that, as expected, the Gal*p* and Glc*p* rings adopt the $^4C_1$ chair conformation, while the Neu*p*5Ac are in the $^2C_4$ conformation. The NMR experiments for the characterization of the oligosaccharides ($^1H—^{13}C$ HSQC, TOCSY, NOESY) were acquired at 298 K with Bruker Avance II 600 MHz spectrometer (Bruker Inc.;Billerica, MA, US) equipped with PATXI probes. The NMR samples (1 mg/500 μL) were prepared in D_2O. The spectra were processed and analyzed with the TOPSPIN 2.0 (Bruker) software. ^1H and ^{13}C NMR chemical shift assignments were performed using standard 2D experiments. In particular ^1H-TOCSY (20 ms and 90 ms of mixing times), ^1H-NOESY (50 ms and 100 ms of mixing time), $^1H—^{13}C$ HSQC. All experiments employed 256 t_1-increments of 2 K points each, with a relaxation delay of 1 s. The ^1H dimensions were 7 ppm in TOCSY and NOESY and 10 ppm in HSQC. The ^{13}C dimension was 140 ppm. 32 scans were employed for the NOESY and TOCSY. The HSQC employed either 128 scans (MenC), 72 scans (MenW) or 64 scans (MenY).

For the acquisition of the ^1H-STD-NMR experiments the antibodies were buffer exchanged to deuterated PBS 1× pD 7.8 using centrifuge filters (Sartorius Vivaspin 650,000 MWCO). Proper antibody folding was assessed by means of ^1H NMR spectra (Fig. S11). All the mAbs displayed good chemical shift dispersion, indicative that the tertiary structure was intact. The STD-NMR experiments for MenC were performed using MenC.01 mAb concentrated at 5 μM in the presence of MenC DP6 concentrated 500 μM. The samples for MenW were prepared employing MenW.01 mAb concentrated at 5 μM in the presence of MenW DP5 concentrated 280 μM. The STD-NMR experiments for MenY were performed using MenY.02 mAb concentrated at 4 μM in the presence of MenY DP5 concentrated 280 μM.

The STD experiments were recorded using Bruker AVANCE II 800 MHz NMR spectrometer equipped with cryo-probe (Bruker Inc.; Billerica, MA, US) at 298 K. The *stddiffesgp* sequence was chosen from the Bruker library, which includes spoil and T2 filters and excitation sculpting. The STD NMR spectra were acquired with 2880 scans and 10 s of relaxation delay. Different conditions were screened for STD experiments. All the STD experiments were performed at both on-resonances, at the aliphatic (0 ppm) and aromatic (7 ppm) regions. The resulting STD spectra provided similar results, same STD epitope mapping, yet the overall intensity was higher for aliphatic irradiation (Fig. S12). Thus, the presented results correspond to the STD spectra obtained with protein aliphatic signals irradiation. The on- and off-resonance spectra were registered in the interleaved mode with the same number of scans. The on-resonance protein saturation was obtained using a Gaussian shape pulse of 50 ms with a total saturation time of 2 s at a frequency of δ 0 ppm (aliphatic region). The off-resonance frequency was always set at δ 100 ppm.

Blank STD experiments just with isolated glycan, in the absence of the mAb, have also been tested (Fig. S13). In all the experiments, the final STD-NMR spectra were obtained by subtracting the on-resonance spectrum from the off-resonance spectrum. STD experiments of the free ligands were obtained using the same experimental details used for the mixture and these spectra were subtracted to the STD of the complex, obtaining the STDD (Fig. s14). The weak STD NMR intensities detected in the blank experiments of the ligands are likely due to direct irradiation or slow relaxation effects. No STD signals appeared in the blank experiment performed with the antibodies alone. The analysis was carried out using the ^1H NMR signals of the STD or STDD spectrum and from their comparison with the off-resonance spectrum, the STD-AF (Average Factor) was obtained. The strongest STD intensity was used as reference (100 % of STD effect). On this basis, the relative STD intensities for the other protons were estimated from the comparison of the corresponding integrals. These relative STD intensities (STD%) were used to map the ligand-binding epitope.

4.9. Ab initio calculations

Gaussian09 suite of programs was employed to perform Density Functional Theory (DFT) theoretical calculations. The geometry optimization and the scan analysis were performed using Becke's hybrid three-parameter exchange functional and the nonlocal correlation functional B3LYP with the 6–31++g(d,p) basis set (Becke, 1992). The polarizable continuum model (PCM) for water (IEF-PCM) was used in order to include solvent effects. The electronic energies were used to originate the energy profiles around the dihedral angles of interest.

4.10. Molecular dynamics simulations

MD simulations were performed using AMBER12 (Case et al., 2012) and AMBER16 (Case et al., 2016) with GLYCAM06j-1 force field (Karl N. Kirschner et al., 2008) in explicit water. 1 μs simulations were employed to access to the conformational and dynamic information of MenC, MenY and MenW CPS.

As first step, the natural molecules were built using the GLYCAM carbohydrate builder web tool, including the OAc groups (http://glycam.org). The molecules were solvated in a theoretical box of explicit TIP3P waters and the solute atoms were positioned at least at 10 Å from the solvent box edge and counter ions were added to maintain electro-neutrality. Two consecutive minimization steps were performed involving (1) only the water molecules and ions and (2) the whole system with a higher number of cycles, using the steepest descent algorithm. The system was then heated up to 300 K during 100 ps followed by 2 ns dynamics at constant temperature and pressure (300 K and 1 atm respectively). During the simulations, the SHAKE algorithm (Miyamoto & Kollman, 1992) was applied to all hydrogen atoms. Minimization, equilibration, and production phases were carried out by the pmemd.cuda (Le Grand et al., 2013; Pierce et al., 2012; Salomon-Ferrer et al., 2013) module of AMBER12 and AMBER16, while the analyses of the simulations were performed using cpptraj module from AMBERTOOLS 16. Data processing and 2D plots were carried out using GNUplot software.

4.11. Docking studies

The global minimum conformer obtained from the MD analysis of MenC, MenY and MenW CPS was taken as the starting point to create the DP5 (MenY and MenW) and DP10 (MenC) geometry by elimination of the external residues. The molecule was then solvated in a theoretical box of explicit TIP3P waters; the solute atoms were positioned at least at 10 Å from the solvent box edge, and counterions were added to maintain electroneutrality. The equilibration phase consisted of first an energy minimization of the solvent, followed by an energy minimization of the entire system without restraints. The resulting structure was placed into the CRD of the MenW.01 crystal structure and manually docked to maximize the intermolecular interactions. The docked structures were then submitted to energy minimization with a low gradient convergence threshold (0.05) in 5000 steps. The OPLS_2005 force field was employed, as integrated in the MAESTRO (Schroedinger) suite of programs. All figures were generated using the molecular graphic software PyMOL (The PyMOL Molecular Graphics System, Version 2.4 Schrödinger, LLC, http://www.pymol.org).

Ethics statement

BALB/c mice were housed and bred under specific pathogen–free conditions at the Central Animal Facility of the Faculty of Medicine, University of Rijeka. The Ethics Committee at the University of Rijeka and National committee for Welfare of Animals approved experiments.

Funding

This work was supported by GlaxoSmithKline Biologicals and received funding from the European Union's Horizon 2020 Research and Innovation Programme under the Marie Skłodowska Curie Grant Agreement 675671 (to RA); from the University of Rijeka, uniri-iskusni-biomed-23-197 (to TLR); and from 'Strengthening the capacity of CerVirVac for research in virus immunology and vaccinology,' Grant No. KK.01.1.1.01.0006, awarded to the Scientific Centre of Excellence for Virus Immunology and Vaccines and co-financed by the European Regional Development Fund (to SJ).

CRediT authorship contribution statement

Gian Pietro Pietri: Writing – review & editing, Writing – original draft, Investigation, Formal analysis. **Sara Bertuzzi:** Writing – review & editing, Investigation, Formal analysis. **Katarina Karnicar:** Formal analysis. **Luca Unione:** Writing – review & editing, Formal analysis. **Berislav Lisnic:** Formal analysis. **Suzana Malic:** Formal analysis. **Karmela Miklic:** Formal analysis. **Matej Novak:** Formal analysis. **Ilaria Calloni:** Formal analysis. **Laura Santini:** Formal analysis. **Aleksandra Usenik:** Formal analysis. **Maria Rosaria Romano:** Formal analysis. **Roberto Adamo:** Writing – review & editing, Investigation, Funding acquisition. **Stipan Jonjic:** Investigation, Funding acquisition. **Dusan Turk:** Investigation. **Jesús Jiménez-Barbero:** Writing – review & editing, Investigation, Funding acquisition. **Tihana Lenac Rovis:** Writing – review & editing, Investigation, Funding acquisition.

Declaration of generative AI and AI-assisted technologies in the writing process

The corresponding author, TLR, utilized ChatGPT to improve sentence clarity due to a lack of native English speakers on the team. No new information was introduced through the use of AI, and the corresponding author TLR reviewed and assumes full responsibility for the content.

Declaration of competing interest

LS, MRR and RA are employee of GSK. GPP was a PhD fellow of MEDRI and performed a secondment in GSK during his doctorate. Menjugate, Menveo, Menitorix, Menhibrix are registered trademarks from GSK Vaccines; Menactra is a registered trademark from Sanofi Pasteur; Nimenrix is a registered trademark from Pfizer; NeisVac is a registerd trademark from North American Vaccine Inc.- Baxter Bioscience.

Data availability statement

All data supporting the findings of this study are available within the article and its supplementary information. Additionally, all structural data have been deposited in the Protein Data Bank (PDB entry code 8S6E). Raw data are available upon request from the corresponding author. Furthermore, all mouse monoclonal antibodies generated to meningococcal sugars are available upon request.

Appendix A. Supplementary data

Supplementary data to this article can be found online at https://doi.org/10.1016/j.carbpol.2024.122349.

References

Abdelhameed, A. S., Morris, G. A., Almutairi, F., Adams, G. G., Duvivier, P., Conrath, K., & Harding, S. E. (2016). Solution conformation and flexibility of capsular polysaccharides from Neisseria meningitidis and glycoconjugates with the tetanus toxoid protein. *Scientific Reports, 6*(June), 1–11. https://doi.org/10.1038/srep35588

Acevedo, R., Zayas, C., Norheim, G., Fernández, S., Cedré, B., Aranguren, Y., … García, L. (2017). Outer membrane vesicles extracted from Neisseria meningitidis serogroup X for prevention of meningococcal disease in Africa. *Pharmacological Research, 121*, 194–201. https://doi.org/10.1016/j.phrs.2017.04.030

Anderluh, M., Berti, F., Bzducha-Wróbel, A., Chiodo, F., Colombo, C., Compostella, F., … van Vliet, S. J. (2022). Recent advances on smart glycoconjugate vaccines in infections and cancer. *FEBS Journal, 289*(14), 4251–4303. https://doi.org/10.1111/febs.15909

Becke, A. D. (1992). Density-functional thermochemistry. I. The effect of the exchange-only gradient correction. *The Journal of Chemical Physics, 96*(February 1992), 2155–2160.

Berti, F. (2018). Multivalent meningococcal conjugate vaccines: Chemical conjugation strategies used for the preparation of vaccines licensed or in clinical trials. *ACS Symposium Series, 1290*. https://doi.org/10.1021/bk-2018-1290.ch006

Berti, F., De Ricco, R., & Rappuoli, R. (2018). Role of o-acetylation in the immunogenicity of bacterial polysaccharide vaccines. *Molecules, 23*(6), 1–10. https://doi.org/10.3390/molecules23061340

Broecker, F., Hanske, J., Martin, C. E., Baek, J. Y., Wahlbrink, A., Wojcik, F., … Seeberger, P. H. (2016). Multivalent display of minimal Clostridium difficile glycan epitopes mimics antigenic properties of larger glycans. *Nature Communications, 7*. https://doi.org/10.1038/ncomms11224

Bröker, M., Dull, P. M., Rappuoli, R., & Costantino, P. (2009). Chemistry of a new investigational quadrivalent meningococcal conjugate vaccine that is immunogenic at all ages. *Vaccine, 27*(41), 5574–5580. https://doi.org/10.1016/j.vaccine.2009.07.036

Case, D. A., Betz, R. M., Cerutti, D. S., Cheatham, T. E., Darden, T. A., Duke, R. E., … Homeyer, N. (2016). *AMBER 2016 reference manual* (pp. 1–923). San Francisco, CA, USA: University of California.

Case, D. A., Darden, T. A., Cheatham, T. E., III, Simmerling, C. L., Wang, J., Duke, R. E., … Kollman, P. A. (2012). *AMBER 12*. San Francisco: University of California.

Cavalcante, T., Medeiros, M. M., Mule, S. N., Palmisano, G., & Stolf, B. S. (2021). The role of sialic acids in the establishment of infections by pathogens, with special focus on leishmania. *Frontiers in Cellular and Infection Microbiology, 11*(May), 1–13. https://doi.org/10.3389/fcimb.2021.671913

Cohen, D., Atsmon, J., Artaud, C., Meron-Sudai, S., Gougeon, M. L., Bialik, A., … Phalipon, A. (2021). Safety and immunogenicity of a synthetic carbohydrate conjugate vaccine against Shigella flexneri 2a in healthy adult volunteers: A phase 1, dose-escalating, single-blind, randomised, placebo-controlled study. *The Lancet Infectious Diseases, 21*(4), 546–558. https://doi.org/10.1016/S1473-3099(20)30488-6

Colombo, C., Pitirollo, O., & Lay, L. (2018). Recent Advances in the Synthesis of Glycoconjugates for Vaccine Development. *Molecules (Basel, Switzerland), 23*(7). https://doi.org/10.3390/molecules23071712

Costantino, P., Norelli, F., Giannozzi, A., D'Ascenzi, S., Bartoloni, A., Kaur, S., … Ceccarini, C. (1999). Size fractionation of bacterial capsular polysaccharides for their use in conjugate vaccines. *Vaccine, 17*(9–10), 1251–1263. https://doi.org/10.1016/S0264-410X(98)00348-X

Dalal, J., Rana, R., Harale, K., Hanif, S., Kumar, N., Singh, D., & Chhikara, M. K. (2019). Development and pre-clinical evaluation of a synthetic oligosaccharide-protein conjugate vaccine against Neisseria meningitidis serogroup C. *Vaccine, 37*(36), 5297–5306. https://doi.org/10.1016/j.vaccine.2019.07.053

Emmadi, M., Khan, N., Lykke, L., Reppe, K., Parameswarappa, S. G., Lisboa, M. P., … Seeberger, P. H. (2017). A Streptococcus pneumoniae type 2 oligosaccharide Glycoconjugate elicits opsonic antibodies and is protective in an animal model of invasive pneumococcal disease. *Journal of the American Chemical Society, 139*(41), 14783–14791. https://doi.org/10.1021/jacs.7b07836

Emsley, P., & Cowtan, K. (2004). Coot: Model-building tools for molecular graphics. *Acta Crystallographica Section D: Biological Crystallography, 60*(12 I), 2126–2132. https://doi.org/10.1107/S0907444904019158

Eneva, R., Engibarov, S., Abrashev, R., Krumova, E., & Angelova, M. (2021). Sialic acids, sialoconjugates and enzymes of their metabolism in fungi. *Biotechnology & Biotechnological Equipment, 35*(1), 364–375. https://doi.org/10.1080/13102818.2021.1879678

Enotarpi, J., Tontini, M., Balocchi, C., van der Es, D., Auberger, L., Balducci, E., … Adamo, R. (2020). A stabilized glycomimetic conjugate vaccine inducing protective antibodies against Neisseria meningitidis serogroup A. *Nature Communications, 11*(1), 1–9. https://doi.org/10.1038/s41467-020-18279-x

Fiorino, F., Rondini, S., Micoli, F., Lanzilao, L., Alfini, R., Mancini, F., … Medaglini, D. (2017). Immunogenicity of a bivalent adjuvanted glycoconjugate vaccine against salmonella typhimurium and salmonella Enteritidis. *Frontiers in Immunology, 8*(FEB), 1–11. https://doi.org/10.3389/fimmu.2017.00168

Fusco, P. C., Farley, E. K., Huang, C. H., Moore, S., & Michon, F. (2007). Protective meningococcal capsular polysaccharide epitopes and the role of O acetylation. *Clinical and Vaccine Immunology, 14*(5), 577–584. https://doi.org/10.1128/CVI.00009-07

Fusco, P. C., Farley, K., Huang, C. H., Moore, S., Michon, F., Farley, E. K., … Michon, F. (2007). Protective meningococcal capsular polysaccharide epitopes and the role of O acetylation. *Clinical and Vaccine Immunology, 14*(5), 577–584. https://doi.org/10.1128/CVI.00009-07

Ganesh, K., Allam, M., Wolter, N., Bratcher, H. B., Harrison, O. B., Lucidarme, J., … Du Plessis, M. (2017). Molecular characterization of invasive capsule null Neisseria meningitidis in South Africa. *BMC Microbiology, 17*(1), 1–10. https://doi.org/10.1186/s12866-017-0942-5

Giuliani, M. M., Santini, L., Brunelli, B., Biolchi, A., Aricò, B., Di Marcello, F., … Pizza, M. (2005). The region comprising amino acids 100 to 255 of Neisseria meningitidis

lipoprotein GNA 1870 elicits bactericidal antibodies. *Infection and Immunity, 73*(2), 1151–1160. https://doi.org/10.1128/IAI.73.2.1151-1160.2005

Gómez-Redondo, M., Ardá, A., Gimeno, A., & Jiménez-Barbero, J. (2020). Bacterial polysaccharides: Conformation, dynamics and molecular recognition by antibodies. In , *Vols. 35–36*. *Drug discovery today: Technologies* (pp. 1–11). Elsevier Ltd.. https://doi.org/10.1016/j.ddtec.2020.08.002

González, E., Reyes, F., Otero, O., Camacho, F., Cuello, M., Ramírez, F., & Acevedo, R. (2019). Monoclonal antibodies against the capsular polysaccharides A, C, Y, W, and X of Neisseria meningitidis: A platform for the quality control of meningococcal vaccines. *Methods in Molecular Biology, 1969*, 181–203. https://doi.org/10.1007/978-1-4939-9202-7_13

Gudlavalleti, S. K., Lee, C. H., Norris, S. E., Paul-Satyaseela, M., Vann, W. F., & Frasch, C. E. (2007). Comparison of Neisseria meningitidis serogroup W135 polysaccharide-tetanus toxoid conjugate vaccines made by periodate activation of O-acetylated, non-O-acetylated and chemically de-O-acetylated polysaccharide. *Vaccine, 25*(46), 7972–7980. https://doi.org/10.1016/j.vaccine.2007.06.018

Harrison, O. B., Claus, H., Jiang, Y., Bennett, J. S., Bratcher, H. B., Jolley, K. A., … Maiden, M. C. J. (2013). Description and nomenclature of Neisseria meningitidis capsule locus. *Emerging Infectious Diseases, 19*(4), 566–573. https://doi.org/10.3201/eid1904.111799

Henriques, P., Dello, L., Gimeno, A., Biolchi, A., Rosaria, M., & Arda, A. (2020). *Structure of a protective epitope reveals the importance of acetylation of Neisseria meningitidis serogroup A capsular polysaccharide*. https://doi.org/10.1073/pnas.2011385117

Kaplonek, P., Khan, N., Reppe, K., Schumann, B., Emmadi, M., Lisboa, M. P., … Seeberger, P. H. (2018). Improving vaccines against Streptococcus pneumoniae using synthetic glycans. *Proceedings of the National Academy of Sciences of the United States of America, 115*(52), 13353–13358. https://doi.org/10.1073/pnas.1811862115

Kensinger, R., & Arunachalam, A. B. (2022). Preclinical development of the quadrivalent meningococcal (ACYW) tetanus toxoid conjugate vaccine, MenQuadfi®. *Glycoconjugate Journal, 39*(3), 381–392. https://doi.org/10.1007/s10719-022-10050-2

Khatun, F., Dai, C. C., Rivera-Hernandez, T., Hussein, W. M., Khalil, Z. G., Capon, R. J., … Stephenson, R. J. (2021). Immunogenicity assessment of cell wall carbohydrates of Group A Streptococcus via self-adjuvanted glyco-lipopeptides. *ACS Infectious Diseases, 7*(2), 390–405. https://doi.org/10.1021/acsinfecdis.0c00722

Khatun, F., Stephenson, R. J., & Toth, I. (2017). An overview of structural features of antibacterial glycoconjugate vaccines that influence their immunogenicity. *Chemistry - A European Journal, 23*(18), 4233–4254. https://doi.org/10.1002/chem.201603599

Kirschner, K. N., & Woods, R. J. (2001). Solvent interactions determine carbohydrate conformation. *Proceedings of the National Academy of Sciences of the United States of America, 98*(19), 10541–10545. https://doi.org/10.1073/pnas.191362798

Kirschner, K. N., Yongye, A. B., Tschampel, S. M., González-Outeiriño, J., Daniels, C. R., Foley, B. L., & Woods, R. J. (2008). GLYCAM06: A generalizable biomolecular force field. Carbohydrates. *Journal of Computational Chemistry, 29*(4). https://doi.org/10.1002/jcc.20820

Kuttel, M. M., Timol, Z., & Ravenscroft, N. (2017). Cross-protection in Neisseria meningitidis serogroups Y and W polysaccharides: A comparative conformational analysis. *Carbohydrate Research, 446–447*, 40–47. https://doi.org/10.1016/j.carres.2017.05.004

Le Grand, S., Götz, A. W., & Walker, R. C. (2013). SPFP: Speed without compromise - a mixed precision model for GPU accelerated molecular dynamics simulations. *Computer Physics Communications, 184*(2), 374–380. https://doi.org/10.1016/j.cpc.2012.09.022

Lee, H. J., Rakic, B., Gilbert, M., Wakarchuk, W. W., Withers, S. G., & Strynadka, N. C. J. (2009). Structural and kinetic characterizations of the polysialic acid O-acetyltransferase OatWY from Neisseria meningitidis. *Journal of Biological Chemistry, 284*(36), 24501–24511. https://doi.org/10.1074/jbc.M109.006049

Li, Y., & Chen, X. (2012). Sialic acid metabolism and sialyltransferases: Natural functions and applications. *Applied Microbiology and Biotechnology, 94*(4), 887–905. https://doi.org/10.1007/s00253-012-4040-1

Liao, G., Zhou, Z., & Guo, Z. (2015). Synthesis and immunological study of α-2,9-oligosialic acid conjugates as anti-group C meningitis vaccines. *Chemical Communications, 51*(47), 9647–9650. https://doi.org/10.1039/c5cc01794g

Liao, G., Zhou, Z., Suryawanshi, S., Mondal, M. A., & Guo, Z. (2016). Fully synthetic self-adjuvanting a-2,9-oligosialic acid based conjugate vaccines against group C meningitis. *ACS Central Science, 2*(4), 210–218. https://doi.org/10.1021/acscentsci.5b00364

Liebschner, D., Afonine, P. V., Baker, M. L., Bunkoczi, G., Chen, V. B., Croll, T. I., … Adams, P. D. (2019). Macromolecular structure determination using X-rays, neutrons and electrons: Recent developments in Phenix. *Acta Crystallographica Section D: Structural Biology, 75*, 861–877. https://doi.org/10.1107/S2059798319011471

Lindič, N., Loboda, J., Usenik, A., Vidmar, R., & Turk, D. (2020). The structure of clostridioides difficile seca2 atpase exposes regions responsible for differential target recognition of the seca1 and seca2-dependent systems. *International Journal of Molecular Sciences, 21*(17), 1–17. https://doi.org/10.3390/ijms21176153

Madariaga, S., Cedré, B., García, M., González, E., & Va, F. (2018). *Evaluation of Bactericidal Activity of Monoclonal Antibodies Obtained from Clinical Infectious Diseases: Open Access Evaluation of Bactericidal Activity of Monoclonal Antibodies Obtained from Neisseria meningitidis. 2(January 2019)* pp. 2–5).

Maiden, M. C. J. (2013). The impact of protein-conjugate polysaccharide vaccines: An endgame for meningitis? *Philosophical Transactions of the Royal Society B: Biological Sciences, 368*(1623). https://doi.org/10.1098/rstb.2012.0147

Martin, C. E., Broecker, F., Oberli, M. A., Komor, J., Mattner, J., Anish, C., & Seeberger, P. H. (2013). Immunological evaluation of a synthetic clostridium difficile oligosaccharide conjugate vaccine candidate and identification of a minimal epitope. *Journal of the American Chemical Society, 135*(26), 9713–9722. https://doi.org/10.1021/ja401410y

Mayer, M., & Meyer, B. (1999). Characterization of ligand binding by saturation transfer difference NMR spectroscopy. *Angewandte Chemie - International Edition, 38*(12), 1784–1788. https://doi.org/10.1002/(SICI)1521-3773(19990614)38:12<1784::AID-ANIE1784>3.0.CO;2-Q

Micoli, F., Del Bino, L., Alfini, R., Carboni, F., Romano, M. R., & Adamo, R. (2019). Glycoconjugate vaccines: Current approaches towards faster vaccine design. *Expert Review of Vaccines, 18*(9), 881–895. https://doi.org/10.1080/14760584.2019.1657012

Micoli, F., Romano, M. R., Tontini, M., Cappelletti, E., Gavini, M., Proietti, D., … Costantino, P. (2013). Development of a glycoconjugate vaccine to prevent meningitis in Africa caused by meningococcal serogroup X. *Proceedings of the National Academy of Sciences of the United States of America, 110*(47), 19077–19082. https://doi.org/10.1073/pnas.1314476110

Micoli, F., Stefanetti, G., & MacLennan, C. A. (2023). Exploring the variables influencing the immune response of traditional and innovative glycoconjugate vaccines. *Frontiers in Molecular Biosciences, 10*(May), 1–19. https://doi.org/10.3389/fmolb.2023.1201693

Mitra, S., & Tomar, P. C. (2021). Hybridoma technology; advancements, clinical significance, and future aspects. *Journal of Genetic Engineering and Biotechnology, 19*(1). https://doi.org/10.1186/s43141-021-00264-6

Miyamoto, S., & Kollman, P. A. (1992). Settle: An analytical version of the SHAKE and RATTLE algorithm for rigid water models. *Journal of Computational Chemistry, 13*(8), 952–962. https://doi.org/10.1002/jcc.540130805

Moore, S. L., Uitz, C., Ling, C. C., Bundle, D. R., Fusco, P. C., & Michon, F. (2007). Epitope specificities of the group Y and W-135 polysaccharides of Neissena meningitidis. *Clinical and Vaccine Immunology, 14*(10), 1311–1317. https://doi.org/10.1128/CVI.00049-07

Mulard, L. A. (2018). Bacterial polysaccharides as major surface antigens: Interest in O-acetyl substitutions. *Carbohydrate chemistry, 43*, 71–103. https://doi.org/10.1039/9781788010641-00071

Nettleship, J. E., Ren, J., Rahman, N., Berrow, N. S., Hatherley, D., Neil Barclay, A., & Owens, R. J. (2008). A pipeline for the production of antibody fragments for structural studies using transient expression in HEK 293T cells. *Protein Expression and Purification, 62*(1), 83–89. https://doi.org/10.1016/j.pep.2008.06.017

Oldrini, D., del Bino, L., Arda, A., Carboni, F., Henriques, P., Angiolini, F., … Adamo, R. (2020). Structure-Guided Design of a Group B Streptococcus Type III Synthetic Glycan–Conjugate Vaccine. *Chemistry - A European Journal, 26*(31), 7018–7025. https://doi.org/10.1002/chem.202000284

Pierce, L. C. T., Salomon-Ferrer, R., De, A. F., Oliveira, C., McCammon, J. A., & Walker, R. C. (2012). Routine access to millisecond time scale events with accelerated molecular dynamics. *Journal of Chemical Theory and Computation, 8*(9), 2997–3002. https://doi.org/10.1021/ct300284c

Pietri, G. P., Tontini, M., Brogioni, B., Oldrini, D., Robakiewicz, S., Henriques, P., … Adamo, R. (2021). Elucidating the structural and minimal protective epitope of the serogroup X meningococcal capsular polysaccharide. *Frontiers in Molecular Biosciences, 8*(October), 1–16. https://doi.org/10.3389/fmolb.2021.745360

Pintar, S., Borišek, J., Usenik, A., Perdih, A., & Turk, D. (2020). Domain sliding of two Staphylococcus aureus N-acetylglucosaminidases enables their substrate-binding prior to its catalysis. *Communications Biology, 3*(1), 1–9. https://doi.org/10.1038/s42003-020-0911-7

Purmohamad, A., Abasi, E., Azimi, T., Hosseini, S., Safari, H., Nasiri, M. J., & Imani Fooladi, A. A. (2019). Global estimate of Neisseria meningitidis serogroups proportion in invasive meningococcal disease: A systematic review and meta-analysis. *Microbial Pathogenesis, 134*(June), Article 103571. https://doi.org/10.1016/j.micpath.2019.103571

Safari, D., Marradi, M., Chiodo, F., Th Dekker, H. A., Shan, Y., Adamo, R., … Snippe, H. (2012). Gold nanoparticles as carriers for a synthetic Streptococcus pneumoniae type 14 conjugate vaccine. *Nanomedicine, 7*(5). https://doi.org/10.2217/nnm.11.151

Salomon-Ferrer, R., Götz, A. W., Poole, D., Le Grand, S., & Walker, R. C. (2013). Routine microsecond molecular dynamics simulations with AMBER on GPUs. 2. Explicit solvent particle mesh ewald. *Journal of Chemical Theory and Computation, 9*(9), 3878–3888. https://doi.org/10.1021/ct400314y

Schneider, M. C., Exley, R. M., Ram, S., Sim, R. B., & Tang, C. M. (2007). Interactions between Neisseria meningitidis and the complement system. *Trends in Microbiology, 15*(5), 233–240. https://doi.org/10.1016/j.tim.2007.03.005

Schumann, B., Hahm, H. S., Parameswarappa, S. G., Reppe, K., Wahlbrink, A., Govindan, S., … Seeberger, P. H. (2017). A semisynthetic Streptococcus pneumoniae serotype 8 glycoconjugate vaccine. *Science Translational Medicine, 9*(380). https://doi.org/10.1126/scitranslmed.aaf5347

Severi, E., Hood, D. W., & Thomas, G. H. (2007). Sialic acid utilization by bacterial pathogens. *Microbiology, 153*(9), 2817–2822. https://doi.org/10.1099/mic.0.2007/009480-0

Trattnig, N., Li, Z., Bosman, G. P., Kosma, P., & Boons, G. J. (2022). Site-specific multi-functionalization of the carrier protein CRM197 by disulfide rebridging for conjugate vaccine development. *ChemBioChem, 23*(21), 1–8. https://doi.org/10.1002/cbic.202200408

Tsang, R. S. W., & Zollinger, W. D. (2005). Serological specificities of murine hybridoma monoclonal antibodies against Neissena meningitidis serogroups B, C, Y, and W135 and evaluation of their usefulness as serogrouping reagents by indirect whole-cell enzyme-linked immunosorbent assay. *Clinical and Diagnostic Laboratory Immunology, 12*(1), 152–156. https://doi.org/10.1128/CDLI.12.1.152-156.2005

Usenik, A., Renko, M., Mihelič, M., Lindič, N., Borišek, J., Perdih, A., … Turk, D. (2017). The CWB2 cell wall-anchoring module is revealed by the crystal structures of the clostridium difficile cell wall proteins Cwp8 and Cwp6. *Structure, 25*(3), 514–521. https://doi.org/10.1016/j.str.2016.12.018

Valverde, P., Ardá, A., Reichardt, N. C., Jiménez-Barbero, J., & Gimeno, A. (2019). Glycans in drug discovery. *MedChemComm, 10*(10), 1678–1691. https://doi.org/10.1039/c9md00292h

Valverde, P., Quintana, J. I., Santos, J. I., Ardá, A., & Jiménez-Barbero, J. (2019). Novel NMR avenues to explore the conformation and interactions of glycans. *ACS Omega, 4*(9), 13618–13630. https://doi.org/10.1021/acsomega.9b01901

Vulliez-Le Normand, B., Saul, F. A., Phalipon, A., Bélot, F., Guerreiro, C., Mulard, L. A., & Bentley, G. A. (2008). Structures of synthetic O-antigen fragments from serotype 2a Shigella flexneri in complex with a protective monoclonal antibody. *Proceedings of the National Academy of Sciences of the United States of America, 105*(29), 9976–9981. https://doi.org/10.1073/pnas.0801711105

Wang, C. H., Li, S. T., Lin, T. L., Cheng, Y. Y., Sun, T. H., Wang, J. T., … Wu, C. Y. (2013). Synthesis of Neisseria meningitidis serogroup W135 capsular oligosaccharides for immunogenicity comparison and vaccine development. *Angewandte Chemie - International Edition, 52*(35), 9157–9161. https://doi.org/10.1002/anie.201302540

Zhu, H., Wang, Q., Wen, L., Xu, J., Shao, Z., Chen, M., … Wang, L. (2012). Development of a multiplex PCR assay for detection and genogrouping of Neisseria meningitidis. *Journal of Clinical Microbiology, 50*(1), 46–51. https://doi.org/10.1128/JCM.00918-11